

**ASSESSMENT OF PATIENT DOSES OF ENDOVASCULAR  
EMBOLIZATION OF THE ARTERIOVENOUS VASCULAR  
MALFORMATIONS**

The image features a large, faint watermark of the Mahidol University logo in the background. The logo is circular with a gold border and contains a central emblem with Thai script. The name 'WANLAPA PROMSIRI' is printed in bold black text across the center of the logo.

**WANLAPA PROMSIRI**

**A THESIS SUBMITTED IN PARTIAL FULFILLMENT  
OF THE REQUIREMENTS FOR  
THE DEGREE OF MASTER OF SCIENCE  
(MEDICAL PHYSICS)**

**FACULTY OF GRADUATE STUDIES  
MAHIDOL UNIVERSITY**

**2005**

**ISBN 974-04-6336-3**

**COPYRIGHT OF MAHIDOL UNIVERSITY**

Thesis  
Entitled

**ASSESSMENT OF PATIENT DOSES OF ENDOVASCULAR  
EMBOLIZATION OF THE ARTERIOVENOUS VASCULAR  
MALFORMATIONS**

*Wanlapa Pomsiri*.....

Ms.Wanlapa Pomsiri,  
Candidate

*J. Laothamatas*..... MD.

Assoc.Prof.Jiraporn Laothamatas,  
M.D.  
Major-Advisor

*Sawwanee Asavaphatiboon*.....

Ms.Sawwanee Asavaphatiboon,  
M.Sc.(Medical Physics)  
Co-Advisor

*Paitoon Tawsagul*.....

Mr.Paitoon Tawsagul,  
M.Sc.(Medical Physics)  
Co-Advisor

*Rassmidara Hoonsawat*.....

Assoc.Prof.Rassmidara Hoonsawat,  
Ph.D.  
Dean  
Faculty of Graduate Studies

*Vipa Boonkittichatoen*.....

Assoc.Prof.Vipa Boonkittichatoen,  
Ph.D.(Radiation Biology)  
Chair  
Master of Science Programme  
in Medical Physics  
Faculty of Medicine,  
Ramathibodi Hospital

Thesis

Entitled

**ASSESSMENT OF PATIENT DOSES OF ENDOVASCULAR  
EMBOLIZATION OF THE ARTERIOVENOUS VASCULAR  
MALFORMATIONS**

was submitted to the Faculty of Graduate Studies, Mahidol University  
for the degree of Master of Science (Medical Physics)

on

July 8, 2005

*Wanlapa Pomsiri*  
.....

Ms. Wanlapa Pomsiri

Candidate

*Sawwane Asavaphatiboon*  
.....

Ms. Sawwane Asavaphatiboon,

M.Sc. (Medical Physics)

Member

*Jiraporn Laothamatas*  
.....

Assoc. Prof. Jiraporn Laothamatas,

M.D.

Chair

*Paitoon Tawsagul*  
.....

Mr. Paitoon Tawsagul,

M.Sc. (Medical Physics)

Member

*Somkiat Techanorarach*  
.....

Dr. Somkiat Techanorarach,

M.D.

Member

*Rassmidara Hoonsawat*  
.....

Assoc. Prof. Rassmidara Hoonsawat,  
Ph.D.

Dean

Faculty of Graduate Studies  
Mahidol University

*Rajata Rajatanavin*  
.....

Prof. Rajata Rajatanavin,  
M.D., F.A.C.E.

Professor of Medicine,

Dean,

Faculty of Medicine

Ramathibodi Hospital,

Mahidol University.

## ACKNOWLEDGEMENT

I would like to express my sincere gratitude and deep appreciation to my advisor, Assoc. Prof. Dr. Jiraporn Laothamatas, for her endless kindness, supervision, teaching, suggestion, helpful criticisms, guidance and encouragement throughout the course of graduate program which have enabled me to carry out the study successfully.

My special appreciation is expressed to my co-advisors, Miss Sawwanee Asavaphatiboon and Mr. Paitoon Tawsagul for their valuation criticisms, comments, consultations, stimulations, kindness and generous assistance.

A special thankful to Dr. Napapong Pongnapang for his comments, consultations, and generous assistance.

I am indebted to Assoc. Prof. Dr. Sirinthara Pongpetch and Dr. Pakorn Jiarakongmun for their kindly helps, co-operations and suggestions.

I would like to extend my gratefulness to all the staff of the Department of Radiology, Ramathibodi hospital, Mahidol University for their kindly helps and suggestions.

I am also indebted to the Department of Radiology, Ramathibodi hospital, Mahidol University for allowing the use of their machines in this study.

A special word of thanks is extended to all my teachers of Medical Physics, Faculty of Medicine, Ramathibodi hospital, Mahidol University for their teaching, help suggestion, encouragement and providing an invaluable experience throughout my graduate training program.

Finally, I wish to express my deepest appreciation to my family, my mother, who have been given me endless support, patience, understanding, encouragement, hope, care and love throughout my study.

Wanlapa Promsiri

**ASSESSMENT OF PATIENT DOSES OF ENDOVASCULAR EMBOLIZATION OF THE ARTERIOVENOUS VASCULAR MALFORMATIONS****WANLAPA PROMSIRI 4436398 RAMP/M****M.Sc.(MEDICAL PHYSICS)****THESIS ADVISORS : JIRAPORN LAOTHAMATAS, M.D., SAWWANEE ASAVAPHATIBOON, M.Sc.( MEDICAL PHYSICS), PAITON TAWSAGUL, M.Sc.( MEDICAL PHYSICS)****ABSTRACT**

In the Ramathibodi hospital , the number of patients who underwent endovascular embolization of the arteriovenous vascular malformations procedures increased by nearly 14 % in 2003, and this increasing trend continues. However, no studies have investigated radiation doses from endovascular embolization of the arteriovenous vascular malformations procedures. The purpose of this study was to assess patient doses and the factors which impact on patient doses. The assessment of patient doses were measured in thirty patients by using LiF:Mg,Cu,P thermoluminescent dosimeters (TLD-100H).These were used to measure the entrance skin doses and exit doses in different points of the patients' skin. Entrance skin dose values were converted to effective doses. The highest doses were delivered to the eye. The median entrance skin doses of the eye was 805.22 (range of 40.20 mGy to 1310.05 mGy) for the frontal plane and 110.72 mGy (range of 1.54 mGy to 170 mGy) for the lateral plane. None of the thirty patients reported acute skin injuries and none were observed. The patient doses were affected by multiple technical factors associated with fluoroscopy and radiography mode. However, the influence of radiography mode has the major impact on patient doses.

**KEY WORDS : PATIENT DOSES / TLD / EMBOLIZATION / AVMs****65 P. ISBN 974-04-6336-3**

การประเมินปริมาณรังสีของผู้ป่วยในระหว่างการทำ ENDOVASCULAR EMBOLIZATION ของโรค ARTERIOVENOUS VASCULAR MALFORMATIONS (ASSESSMENT OF PATIENT DOSES OF ENDOVASCULAR EMBOLIZATION OF THE ARTERIOVENOUS VASCULAR MALFORMATIONS)

วัลลภา พรหมศิริ 4436398 RAMP/M

วท.ม. (ฟิสิกส์การแพทย์)

คณะกรรมการควบคุมวิทยานิพนธ์ : จิรพร เหล่าธรรมทัศน์, M.D., เสาวนีย์ อัสวชาติบุญ, M.Sc.(Medical Physics) , ไพฑูร ท้าวสกุล , M.Sc.(Medical Physics)

#### บทคัดย่อ

ในปี พ.ศ. 2546 ผู้ป่วยที่ทำ embolization ของโรค arteriovenous vascular malformations (AVMs) ในโรงพยาบาลรามาธิบดีมีจำนวนเพิ่มขึ้นร้อยละ 14 และมีแนวโน้มจะเพิ่มสูงขึ้นอีกเรื่อยๆ อย่างไรก็ตามไม่พบว่ามีการศึกษาถึงปริมาณรังสีที่เกิดขึ้นในระหว่างการทำ embolization ของโรค AVMs ในโรงพยาบาลรามาธิบดี ดังนั้นในการทดลองครั้งนี้จึงมีจุดประสงค์เพื่อประเมินปริมาณรังสีที่ผู้ป่วยได้รับ และศึกษาถึงปัจจัยต่างๆที่มีผลกระทบต่อปริมาณรังสีที่ผู้ป่วยได้รับในระหว่างการทำ embolization ของโรค AVMs ในโรงพยาบาลรามาธิบดี โดยใช้ LiF:Mg,Cu,P (TLD-100H) เป็นเครื่องมือในการประเมินปริมาณรังสีของผู้ป่วย 30 คน โดยทำการติด TLD-100H ไว้บริเวณผิวของผู้ป่วยที่ตรงกับตำแหน่งของอวัยวะสำคัญต่างๆ เพื่อหาค่า entrance skin dose, exit dose และ effective dose จากการประเมินปริมาณรังสีพบว่าค่าเป็นอวัยวะที่ได้รับปริมาณรังสีสูงสุด โดยค่ากลางของ entrance skin dose ที่ค่ามีค่า 805.22 (40.20 - 1310.05 mGy) สำหรับแนวด้านหน้า และ 110.72 mGy (1.54 - 170 mGy) สำหรับแนวด้านข้าง จากการทดลองนี้ไม่พบว่ามีผู้ป่วยคนใดเกิดความเสียหายบริเวณผิวอย่างเฉียบพลัน เช่น การเกิดผื่นแดงบริเวณผิว ปริมาณรังสีที่ผู้ป่วยได้รับเกิดจากปัจจัยหลายอย่างที่เกี่ยวข้องกับ fluoroscopy mode และ radiography mode ซึ่งปัจจัยที่มีผลต่อปริมาณรังสีที่ผู้ป่วยได้รับมากที่สุดเกิดจากปัจจัยใน radiography mode

65 หน้า ISBN 974-04-6336-3

## CONTENTS

	Page
ACKNOWLEDGEMENT	iii
ABSTRACT	iv
LIST OF TABLES	vii
LIST OF FIGURES	viii
LIST OF ABBREVIATIONS	x
CHAPTER	
I INTRODUCTION	1
II OBJECTIVE	24
III LITERATURE REVIEW	25
IV MATERIALS AND METHODS	27
V RESULTS AND DISCUSSION	34
VI CONCLUSION	61
REFERENCES	62
BIOGRAPHY	65

## LIST OF TABLES

	Page
Table1.1 ICRP 26 and ICRP 60 tissue weighting factors	6
Table1.2 Nuclear Regulatory Commission (NRC) regulatory requirements : Maximum permissible dose equivalent limits	11
Table1.3 Potential effects of fluoroscopic exposures on the reaction of skin and lens of the eye	13
Table1.4 Properties of TL dosimeters commonly used in medicine	21
Table5.1 Correction Factor (CF) for sensitivity of each groups of TLD	35
Table5.2 Summary of technical parameters for endovascular embolization of AVMs procedures	40
Table 5.3 The entrance skin dose and exit dose	45
Table5.4 Effective dose values for frontal plane and lateral plane	51

## LIST OF FIGURES

	Page
Figure 1.1	7
Indirect methods of calculating organ dose depend on (a) the skin dose and percent depth dose data or (b) use of tissue air ratio correction factors.	
Figure1.2	19
Energy-level diagram of the thermoluminescence process : (A) ionization by radiation, and trapping of electrons and holes; (B) heating to release electrons, allowing luminescence production	
Figure1.3	22
Glow curve of LiF: Mg,Cu,P detectors (pre-irradiation annealed at 240 °C for 10 minutes, heating rate 2°C.s <sup>-1</sup> , D = 1.5 mGy)	
Figure1.4	22
The relative TL emission spectra of LiF: Mg,Cu,P	
Figure 4.1	29
TOSHIBA DFP-2000A digital fluorography system	
Figure 4.2	29
The rods of thermoluminescence dosimeter (TLD-100H)	
Figure 4.3	30
TLD annealing oven manufactured by Harshaw Bicon, Solon Ohio, USA	
Figure 4.4	30
Harshaw TLD reader model 5500	
Figure 4.5	31
The Sr-90 dosimeter irradiator model 2000-DI by Harshaw nuclear system	
Figure 5.1	36
The calibration curve of TL signals for absorbed doses of 0.034 mGy to 3.43 mGy	
Figure 5.2	36
The calibration curve of TL signals for absorbed doses of 3.43 mGy to 102.90 mGy	
Figure 5.3	54
The maximum, median and minimum entrance skin dose of each organ for frontal plane	
Figure 5.4	54
The maximum, median and minimum entrance skin dose of each organ for lateral plane	
Figure 5.5	55
The maximum, median and minimum exit dose of each organ for frontal plane	

**LIST OF FIGURES (Continued)**

	Page
Figure 5.6 The maximum, median and minimum exit dose of each organ for lateral plane	55
Figure 5.7 Effective dose of each organ for frontal plane	56
Figure 5.8 Effective dose of each organ for frontal plane	56



## LIST OF ABBREVIATIONS

Abbreviation	Term
AAPM	American Association of Physicist in Medicine
AEC	Automatic exposure control
AP	anterior-posterior
AVM	Arteriovenous malformation
BSF	Backscatter fraction
CaF <sub>2</sub>	Calcium fluoride
CaSO <sub>4</sub>	Calcium sulphate
cGy	Centigray
μGy	Microgray
cm	Centimeter
Co-60	Cobalt-60
°C	Degree Celsius
°C.s <sup>-1</sup>	Degree Celsius per second
CT	Computed Tomography
Cu	Copper
DAP	Dose area product
EAP	Exposure area product
FOV	Field of view
g/cm <sup>3</sup>	gram per cubic centimeter
h	Hour
ICRP	International Commission on Radiological Protection
keV	Kiloelectron Volt
kV	Tube voltage
LiBO <sub>4</sub>	Litium borate
LiF	Litium fluoride
mAs	Tube current
MeV	Megaelectron Volt

## LIST OF ABBREVIATIONS (Continued)

Abbreviation	Term
Mg	Magnesium
min	Minute
mm	Millimeter
mrem	Millirem
mR/rev	Milliroentgen per revolution
mSv	Millisievert
nC	Nanocoulomb
nm	Nanometer
NRC	Nuclear Regulatory Commission
P	Phosphorus
PA	posterior-anterior
R <sup>2</sup>	The correlation coefficient
SID	Source-intensifier distance
SSD	Source to surface distance
Sr-90	Strontium-90
μSv	Microsievert
TAR	Tissue air ratio
Ti	Titanium
TL	Thermoluminescent
TLD	Thermoluminescence dosimeter
w	Week
yr	Year

# CHAPTER I

## INTRODUCTION

### 1.1 Introduction

The number of interventional neuroradiology procedures performed in different countries has increased in recent years (1). This is largely associated with the introduction of new equipment with improved imaging capabilities. These procedure studies the vasculature and potential pathologies of the brain by means of catheterization performed with the transfemoral artery technique. Most interventional neuroradiology procedures are considered of a diagnostic nature where the objective is to identify a neurologic problem. An increasing proportion of interventional neuroradiology procedures may be categorized as therapeutic, where the procedure is undertaken to treat a neurologic condition (2).

Imaging in interventional neuroradiology is normally accomplished by use of fluoroscopy and digital subtraction angiography (DSA). Some of the equipment used in interventional neuroradiology incorporates the latest technical advances in imaging systems and processing acquisition of images. Technical parameters are selected in an automatic or semiautomatic way, while the radiation field size and the focus-to-skin distance depend on the radiologist's preference. In general, neuroradiologic procedures require good image quality, long fluoroscopic times and a large number of angiographic images to visualize and evaluate any vascular pathology (3,4,5). As a result, the amount of radiation received by the patient is a matter of major concern. It is generally accepted that interventional radiology exposes individual patients to the greatest doses of ionizing radiation from medical applications, other than radiation oncology (6). Interventional radiology procedures may involve a risk of radiation induced injury to the patient (7). One interventional neuroradiology procedure that involves high radiation doses to patients is cerebral embolization. It is used for the occlusion of aneurysms and/or arteriovenous malformation embolizations (AVMs)

from the blood supply, which is an accepted complement or alternative to other treatment methods such as surgery and irradiation and allow minimally invasive treatment that is less traumatic to the patient in comparison with surgery. These procedure is also less expensive, since they are associated with a shorter post procedural hospital stay (3).

In Ramathibodi hospital, the number of patients who underwent interventional neuroradiology procedures has increased nearly 14 % in 2003 and this increasing trend continues. However, no studies have investigated radiation doses from endovascular embolization of the arteriovenous vascular malformations procedures gave any information about patient dose and effect that impact on patient dose.

In order to assess the patient dose, the skin (surface) dose is an important dosimetric parameter, as it can be used to predict the possibility of inducing deterministic radiation injuries, such as skin erythema or epilation, and is the key dose parameter whenever the threshold dose for the indication of such injuries is exceeded. It is desirable to keep skin dose below threshold dose for the induction of deterministic effects, which is often taken to be 2 Gy. For radiation doses below the deterministic threshold dose, the patient risk consists of the stochastic risk of carcinogenesis and the induction of genetic effects. Skin dose may be calculated from measured x-ray tube output data, or may be measured using radiation detectors such as thermoluminescent dosimeters (TLDs). Another important dose parameter is the effective dose to the patient. The effective dose takes into account the individual dose and radiosensitivity of all the irradiated organs and tissues. The magnitude of the effective dose is taken to be a measure of the stochastic risks to patients undergoing the specified radiologic examination. The effective dose is generally the most important dosimetric parameter when patient skin doses do not exceed the threshold dose dictating the inducing of deterministic effects (8).

## **1.2 Radiation dosimetry of the patient**

Radiation dosimetry is primarily of interest because radiation dose quantities serve as indices of the risk of biologic damage to the patient. The biologic effects of radiation can be classified as either deterministic or stochastic. Deterministic effects are believed to be caused by cell killing. If a sufficient number of cells in an organ or

tissue are killed, its function can be impaired. Deterministic effects include teratogenic effects to the embryo or fetus, skin damage, and cataracts. For a deterministic effect, a threshold dose can be defined below which the effect will not occur. For doses greater than the threshold dose, the severity of the effect increases with dose. To assess the likelihood of a deterministic effects on an organ from an imaging procedure, the dose to that organ is estimated.

Stochastic effect is caused by damage to a cell that produces genetically transformed but reproductively viable descendants. Cancer and hereditary effects of radiation are considered to be stochastic. The probability of a stochastic effect, instead of its severity, increase with dose. For stochastic effects, there may not be dose thresholds below which the effects cannot occur (8).

In general, the objectives of radiation protection is to prevent deterministic effects and to reduce the likelihood of stochastic effects. Therefore, the strategy of dose monitoring in interventional radiology serves two purposes: 1) to find out which area of the body might receive doses that are comparable with thresholds for deterministic effects in order to keep the radiation dose to them under control; the quantities related to this purpose is the absorbed dose to the most exposed area and 2) to evaluate the quantities related to stochastic effects, in order to keep them as low as reasonably achievable; the quantity related to the overall probability of stochastic effects is the effective dose (9).

### **1.2.1 Effective dose**

The effective dose,  $E$ , is a dosimetry parameter which takes into account the doses received by all irradiated radiosensitive organs and may be taken to be measures of the stochastic risk (9,10). Although the effective dose is an occupational dose quantity based on an age profile for radiation workers, this dose descriptor is being increasingly used to quantify the amount of radiation received by patients undergoing diagnostic examinations which use ionizing radiation. Notwithstanding the fact that there are problems associated with converting effective doses to a corresponding detriment, there are important benefits to be gained by using effective dose to quantify patient doses in diagnostic radiology. One advantage is that the effective dose attempts to measure the risk to the patient, which is the motivation for

all patient dosimetry studies in diagnostic radiology. In addition, the effective dose to a patient undergoing any examination may be compared to that of any other radiologic procedure as well as natural background exposure and regulatory dose limits, which are increasingly expressed using effective dose values (9,10).

### 1.2.1.1 Definitions

#### a) ICRP26 : Effective dose equivalent

In 1977, ICRP Report 26 (9) defined the effective dose equivalent as

$$H_E = \sum W_T \cdot H_T \quad \text{.....Equation 1}$$

Where  $W_T$  is the weighting coefficient per tissue ( $T$ ) or organ

$H_T$  is the dose equivalent to tissue  $T$

$H_E$  is the summation over all tissue of the product  $W_T \cdot H_T$ .

$$H_T = Q \cdot D_T \quad \text{.....Equation 2}$$

Where  $Q$  is the quality factor of the radiation type based on the linear energy transfer (LET) in water ( $Q = 1$  for x-rays)

$D_T$  is the absorbed dose at a point in a given tissue.

The dose equivalent is given the special unit sievert (or rem) to distinguish it from absorbed dose which has the unit gray ( or rad). In 1987, the NCRP adopted this definition of effective dose equivalent, although modifying the values of  $Q$  for neutrons (11).

#### b) ICRP60 : Effective dose

In 1990, ICRP Report 60 (10) recommended three major change for use of the effective dose concept to assess the radiation detriment from nonhomogeneous irradiations. First, they replaced the quality factor  $Q$  with the radiation weighting factor  $W_R$ , which is dependent upon radiation type and energy, independent of organ or tissue type, and determined with guidance from relative biological effectiveness (RBE) data. Second, to determine the dose equivalent for each tissue, the average

tissue dose is used, rather than the radiation weighting dose quantity  $H_T$  is redefined as the equivalent dose (as opposed to the dose equivalent)

$$H_T = \sum W_R \cdot D_{T,R} \dots\dots\dots \text{Equation 3}$$

Where  $W_R$  is the radiation weighting coefficient

$D_{T,R}$  is the average absorbed dose to tissue  $T$

$H_T$  is the summation over all radiation type and energies of the product  $W_R \cdot D_{T,R}$

For x-rays, the value of  $W_R$  is 1. Thus the difference between dose equivalent and equivalent dose is mostly academic (point by point integration of dose over the tissue volume versus a volume averaged dose, respectively). The unit of equivalent dose remains sievert (or rem). Finally, the values for the tissue weighting factor  $W_T$  were modified for several tissues and explicitly defined for others. To differentiate the two definitions, ICRP 60 defines effective dose (as opposed to effective dose equivalent) as

$$E = \sum W_T \cdot H_T = \sum W_T \cdot W_R \cdot D_{T,R} \dots\dots\dots \text{Equation 4}$$

Because of the different weighting coefficients and methods for calculating remainder organ doses (Table1.1), the numerical values of effective dose and effective dose equivalent differ for the same irradiation conditions. In general, due to the greatly reduced contribution of remainder tissues, the value of effective dose is typically lower than that of effective dose equivalent (12).

### 1.2.2 Entrance skin dose

Entrance skin dose (ESD) is an actual measure of radiation received by a portion of the patient's skin (13), which is used to assess the likely severity of deterministic effects, may be measured by means of thermoluminescent dosimeters (TLDs) attached to the patient's skin.

Table 1.1 ICRP 26 and ICRP 60 tissue weighting factors

Organ or tissue	Tissue weighting factor ( $W_T$ )	
	ICRP 26	ICRP 60
Gonad	0.25	0.20
Red bone marrow	0.12	0.12
Colon		0.12
Lung	0.12	0.12
Stomach		0.12
Bladder		0.05
Breast	0.15	0.05
Liver		0.05
Esophagus		0.05
Thyroid	0.03	0.05
Skin	0.01	0.01
Bone surface	0.03	0.01
Remainder	0.30 <sup>a</sup>	0.05 <sup>b</sup>

<sup>a</sup> ICRP 26 remainder organ : A weight of 0.06 is to be assigned to each of the five remainder tissues receiving the highest dose equivalents, and the other remainder tissues or organs are to be neglected. When the GI tract is irradiated, the stomach, small intestine, upper large intestine, and lower large intestine are to be treated as four separate organs and each may therefore be included in the five remainder tissues, depending on the magnitude of the dose equivalent they receive when compared to the dose equivalent received by other remainder tissues and organs. In practice, the remainder organs or tissues are taken to be the five “not specifically listed” organs that receive the highest dose equivalents. The Commission clarified in 1987 that it did not intend the hands and forearms, feet and ankles, skin, and lens of eye to be included in the remainder.

<sup>b</sup> ICRP 60 remainder organ : adrenals , brain , small intestine , kidney , muscle , pancreas , spleen , thymus , uterus , large intestine (removed per 1997 ICRP clarification, to be included with colon). The remainder may also include other tissues or organs selectively irradiated. In those cases in which one of the remainder tissues or organs receives an equivalent dose in excess of the highest dose in any of the 12 organs for which a weighting factor is specified, a weighting factor of 0.025 should be applied to that tissue or organ , and a weighting factor of 0.025 to the average in the other remainder tissues or organ.

### 1.2.3 Organ dose

Organ dose is the dose received by a particular organ. Because organs are not uniform in size, shape, and density, the dose to each part of an organ will differ. The average dose to the irradiated volume is a similar concept that averages the dose received by each portion of tissue contained within the x-ray beam.

The dose to a particular organ will be determined by the x-ray characteristics such as the percentage depth dose, the backscatter fraction (BSF), or alternatively the tissue air ratio (TAR) (figure 1.1). The BSF and TAR can be determined from separate experiments (13).

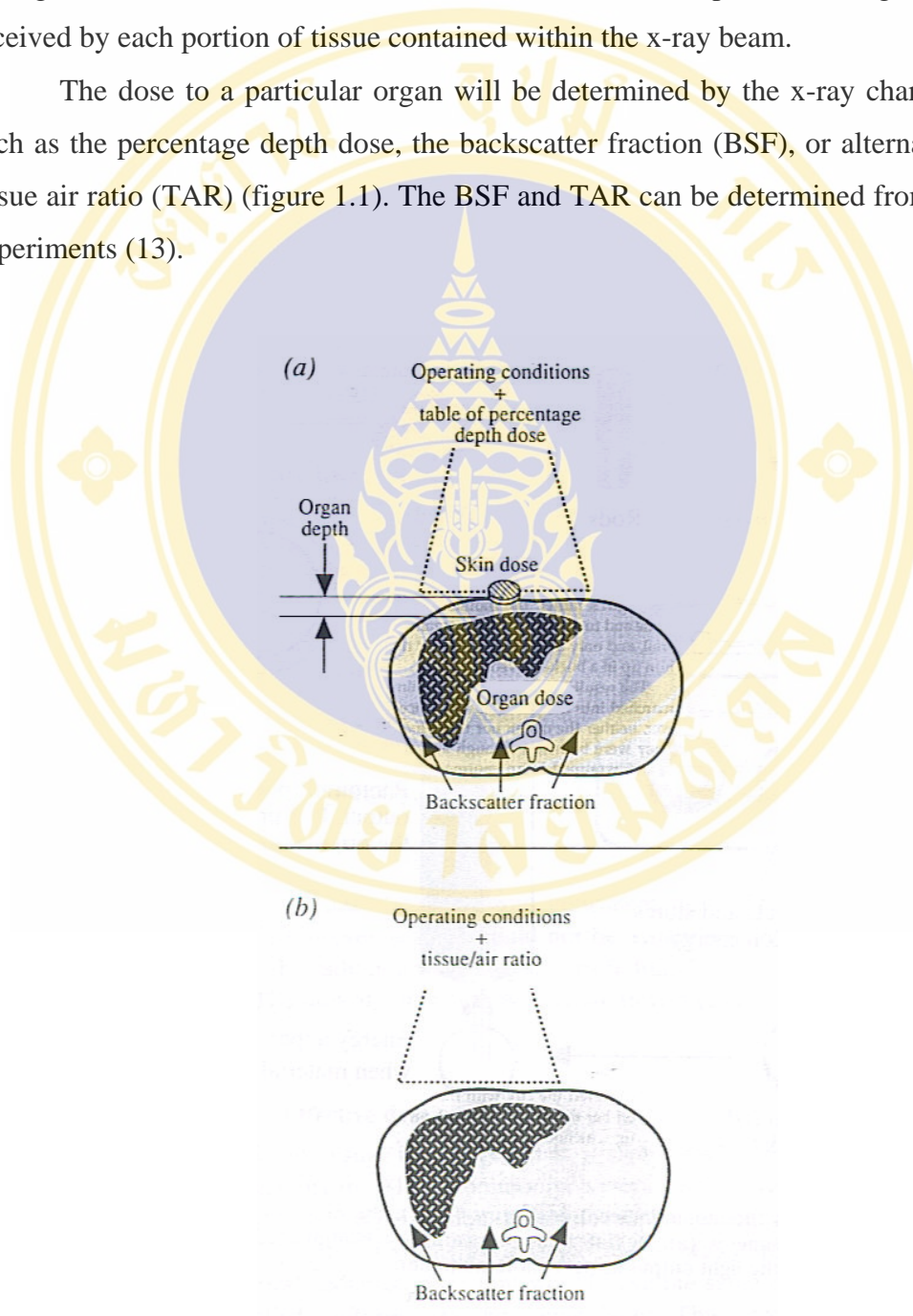


Figure 1.1 Indirect methods of calculating organ dose depend on (a) the skin dose and percent depth dose data or (b) use of tissue air ratio correction factors.

The direct measurements organ dose using TLD dosimeters insert in Rando phantom that mimic the x-ray imaging conditions.

Organ dose were calculated from the formula (14) :

$$D_T = \sum f_{Ti} \cdot D_{Ti}, \dots\dots\dots \text{Equation 5}$$

Where  $D_T$  is the dose to organ/tissue  $T$

$f_{Ti}$  is the fraction of total organ/tissue  $T$  mass in phantom slice  $i$

And  $D_T$  is the average dose to the volume of organ  $T$  lying within phantom slice  $i$ . The dose  $D_{Ti}$  was determined as the mean of the doses monitored by TLDs placed within tissue  $T$  of the Rando phantom slice  $i$ . The  $f_{Ti}$  fraction for all organ for which a tissue weighting factor was specified by ICRP 60 (17). For the brain, thymus, adrenals, spleen, pancreas, kidney, small intestine, and uterus the  $f_{Ti}$  factor were assumed to be the reciprocal of the number of slices that each organ occupies deduced from the organ size reported by ICRP 23 (15).

### 1.3 The methods for patient dosimetry

#### 1.3.1 Calculation of entrance skin dose from calibrated x-ray tube exposure factors

The first method was the use of calibrated exposure factors to calculate the entrance skin dose at the skin surface, using calculations from radiographic and fluoroscopic exposure factors following calibration of the x-ray tube. The calibration procedure consisted of measurement of radiation output under the full range of radiographic and fluoroscopic, including cineangiographic conditions. During interventional neuroradiology procedures, data were recorded such as kV, mAs, time, focus to skin distance. From this information, together with x-ray tube calibration curves, entrance skin dose could be assessed. However, patient dosimetry in interventional neuroradiology procedures is extremely complex due to irradiation of different anatomical areas, with the x-ray beam changing to various projections, focus to skin distance and focus to image intensifier distance. For all these reasons, patient

entrance doses derived from technical parameters such as kV, mA applied during procedure are very difficult to calculate (16).

### 1.3.2 Thermoluminescent dosimeters (TLDs)

This method enables measurement of entrance skin doses and organ dose. Entrance dose measurements either with TLDs attached to the skin of the patient or free in air in the absence of the patient and organ dose were estimated from the dose values monitored by TLDs placed within anthropomorphic phantom.

The main advantages of dose measurements using TLDs are directly dose measurement at the skin surface and organ specific dose determination is allowed and fetal dose measurement is possible. However, this method is remarkably time consuming and labor intensive (17).

### 1.3.3 Dose area product (DAP)

The DAP is a measurement of the radiation dose to air, times and the area of the x-ray field. This method is measured with a flat ionization chamber mounted directly on the light beam diaphragm housing. The DAP ionization chamber must intercept the entire x-ray field for an accurate reading, one proportional to the exposure area product (EAP). The relationship between DAP and EAP is essential a single conversion factor that relates dose to exposure. The reading from DAP meter can be changed by altering the x-ray technique factors (kV, mA or time), varying the area of the field, or both.

DAP is easy to measure and a better indicator of risk than entrance dose alone, since DAP incorporates the entrance dose and field size. DAP has been shown to correlate well with the total energy imparted to the patient, which is related to the effective dose and therefore to overall cancer risk. Consequently, the use of DAP to estimate skin entrance exposure or skin dose is complex and DAP meters are difficult to calibrate and maintain (17).

### 1.3.4 Film dosimetry

The method is based on film dosimetry using Kodak “Ready Pack” film used in radiotherapy departments. The film should be placed on the table underneath the patient for an undercouch tube position. When the interventional neuroradiology procedures originate field distribution much larger than the area covered by the film size, two films could be placed on the table. If the intervention implies lateral projections, also extra films could be employed surrounding the sides of the patient, which is complicate. The characteristic curve can be seen that dose between 10 mGy and 500 mGy could probably be evaluated, but the best fit to a dose response curve is obtained between 20 and 200 mGy. The total cost of the measurement procedure is low.

There are several methods for patient dosimetry, however the common methods for patient dosimetry are measurement of dose area product (DAP) or entrance skin dose by TLDs and effective doses are estimated by multiplication of the measured quantity by conversion factors (18).

### 1.4 Dose Limit

The Nuclear Regulatory Commission (NRC)’s radiation dose limits are intended to limit the risks of stochastic effects, such as cancer and genetic effects, and to prevent deterministic effects such as cataracts, skin damage, sterility and hematologic consequences of bone marrow depletion. To limit the risk of stochastic effects, the sum of the external and internal doses to the entire body, the total effective dose equivalent, may not exceed 50 mSv/yr (5 rem/yr). To prevent deterministic effects, the sum of the external dose and committed dose equivalent to any individual organ (except the lens of the eye) may not exceed 500 mSv/yr (50 rem/yr). The dose to the fetus of a declared pregnant radiation worker may not exceed 5 mSv (0.5 rem) over the 9 month gestational period and should not substantially exceed 500  $\mu$ Sv (50 mrem) in any one month. Table 1.2 lists the most important NRC radiation exposure limits (19).

Table 1.2 Nuclear Regulatory Commission (NRC) regulatory requirements: Maximum permissible dose equivalent limits <sup>a</sup>

Limits	Maximum permissible annual dose limits	
	mSv	rem
<b>Occupational limits</b>		
Total effective dose equivalent	50	5
Total dose equivalent to any individual organ (except lens of eye)	500	50
Dose equivalent to the lens of the eye	150	15
Dose equivalent to the skin or any extremity	500	50
Dose to an embryo/fetus <sup>b</sup>	0.5 in 9 months	0.05 in 9 months
<b>Nonoccupational ( public limits)</b>		
Individual members of the public	1.0/yr	0.1/yr
Unrestricted area	0.02 in any 1 hr <sup>c</sup>	0.002 in any 1 hr <sup>c</sup>

<sup>a</sup> These limits are exclusive of natural background and any dose the individual has received for medical purposes; inclusive of internal committed dose equivalent and external effective dose equivalent (i.e., total effective dose equivalent).

<sup>b</sup> Applies only to conceptus of a worker who declares her pregnancy. If the limit exceeds 4.5 mSv (450 mrem) at declaration, conceptus dose for remainder of gestation is not to exceed 0.5 mSv (50 mrem).

<sup>c</sup> This means the dose to an area (irrespective of occupancy) shall not exceed 0.02 mSv (2 mrem) in any 1 hour. This is not a restriction of instantaneous dose rate to 0.02 mSv/hr (2 mrem/hr).

### 1.5 Radiopathology and radiation risk (10)

Exposure of tissues to x-rays can result in the development of both inflammatory and cell-killing effects or induction of malignancy. The probability of inflammatory and cell-killing effects, of which skin desquamation and ulcers are one

type, is dose-related once the dose exceeds a significant threshold; this threshold for skin is relatively high, but can be exceeded in interventional procedures. Malignancy may occur even at low doses, but the exact dose-response relationship is not accurately known.

Following the irradiation of the skin with single doses of x-rays several distinct waves of radiation response may be seen, depending on the total dose, the dose rate, and the pattern of exposure. The potential risks of skin damage resulting from fluoroscopy have been identified and their time of onset and the associated threshold doses are given in Table 1.3. Without knowing the actual dose rate(s) of various modes of operation, an interventionist can inadvertently reach the thresholds. Columns 4 and 5 of Table 1.3 show the impact of typical (realistic) dose rates in terms of minutes to reach the thresholds. This emphasises the importance of knowing the dose rates being delivered by specific equipment. Any 'rule of thumb', e.g. 100 minutes, should not be used unless it represents the impact of actual dose rates.

The pathophysiological mechanisms leading to the development of many of these changes, which are also seen after radiotherapy or accidental industrial exposure, are now relatively well established. The relationship of the different changes is also now well understood. However, the interpretation of skin changes in an individual case does, to a major extent, require knowledge of the sequence of changes observed. This is not always the situation with reported cases of overexposure in radiological procedures and hence uncertainties as to interpretation exist.

Table 1.3 Potential effects of fluoroscopic exposures on the reaction of skin and lens of the eye

Effect	Approximate threshold dose(Gy)	Time of onset	Minutes of fluoroscopy at typical normal dose rate of 0.02 Gy/min (20mGy/min =2 rad/min) <sup>c</sup>	Minutes of fluoroscopy at typical high dose rate of 0.2 Gy/min (200 mGy/min =20 rad/min) <sup>c</sup>
<b>SKIN <sup>a</sup></b>				
Early transient erythema	2	2-24 h	100	10
Main erythema reaction	6	~ 1.5 w	300	30
Temporary epilation	3	~ 3 w	150	15
Permanent epilation	7	~ 3 w	350	35
Dry desquamation	14	~ 4 w	700	70
Moist desquamation	18	~ 4 w	900	90
Secondary ulceration	24	> 6 w	1200	120
Late erythema	15	8-10 w	750	75
Ischaemic dermal necrosis	18	> 10 w	900	90
Dermal atrophy (1 <sup>st</sup> phase)	10	> 52 w	500	50
Telangiectasis	10	> 52 w	500	50
Dermal necrosis (delayed)	> 12	> 52 w	750	75
Skin cancer	None known	> 15 yr	N/A	N/A
<b>EYE <sup>b</sup></b>				
Lens opacity (detectable)	> 1-2	> 5 yr	> 50 to eye	> 5 to eye
Lens/cataract (debilitating)	> 5	> 5 yr	> 250 to eye	> 25 to eye

<sup>a</sup> Potential effects of fluoroscopic exposures on the reaction of the skin.

Adapted from Wagner and Archer (1998) with reference to Hopewell (1986).

<sup>b</sup> Potential effects of fluoroscopic exposures on the lens. Indicates the doses that can produce detectable but non-symptomatic radiogenic changes and those doses capable of causing significant visual impairment or debilitation.

<sup>c</sup> Without knowing the actual dose rate(s) of various modes of operation, an interventionist can inadvertently reach the thresholds. Columns 4 and 5 show the impact of typical (realistic) dose rates in terms of minutes required to reach the thresholds. This emphasises the importance of knowing the dose rates being delivered by specific equipment. Any 'rule of thumb' e.g. 100 minutes, should not be used, unless it represents the impact of actual dose rates.

## **1.5.1 Radiopathology–skin**

### **1.5.1.1 Early effects**

The first evidence of biologic effects of ionizing radiation appeared on exposed skin in the form of erythema and acute radiation dermatitis. In both patients and medical personnel, exposure of the skin may lead to the development of several waves of erythema or a reddening of the skin. An early response (early transient erythema) is seen a few hours after doses of  $>2$  Gy, when the exposed area is relatively large. This is related to changes in vascular permeability. The main erythematous reaction, whose onset is after approximately 10 days, develops as a consequence of the inflammation secondary to the death of epithelial basal cells. A late wave of erythema may also be seen with an onset at about 8-10 weeks after exposure. This has a bluish tinge and represents dermal ischaemia.

The reaction of the epidermis to radiation exposure is the most extensively documented. The cells most at risk are the basal cells of the epidermis; these are gradually lost after irradiation leading to the development of epidermal hypoplasia within 3-5 weeks of exposure. The severity of the clinical changes that are associated with epidermal hypoplasia depend on the size of the radiation dose. Hypoplasia is identified clinically as either dry desquamation or moist desquamation. The timing depends on the turnover-time of epidermis in the individual patient, but is usually 4–6 weeks after exposure. In cases of very high dose exposure the healing of moist desquamation, a process that depends on cell proliferation and the migration of viable cells, may only occur slowly.

### **1.5.1.2 Late effects**

Late skin changes occur from 26 weeks after irradiation and are characterized by a thinning of dermal tissue, telangiectasia, and the possibility of late necrosis. Telangiectasia is a repeatedly documented late change in human skin after radiotherapy exposure and is rarely seen earlier than 52 weeks. It then increases in both incidence and severity for up to at least 10 y after irradiation. The rate of progression of telangiectasia is dose-related. Late necrosis may be promoted by trauma, or other factors, at any time.

## **1.5.2 Radiopathology–eye**

### **1.5.2.1 Mechanisms**

Ionising radiation can damage a variety of ocular tissues. Many of the effects may be secondary to altered nutrition, e.g., the result of primary effect on the vasculature responsible for aqueous humor production. In the human, the blood-aqueous barrier is somewhat radioresistant, certainly requiring more than a single dose of 5 Gy and perhaps as much as 20 Gy of fractionated doses of x-rays to facilitate breakdown. However, when this occurs, the resulting altered intraocular environment can adversely affect the lens, cornea, and intraocular pressure. If these effects persist, as can happen following fractionated doses of 30–40 Gy delivered in 3–4 days, permanent visual disability can be the outcome.

Except for direct effects on the lens, effects on the vasculature generally mediate the major influence of radiation on the eye. Many radiopathies of the eye require relatively high single or fractionated doses and become apparent only after extended latent periods. The notable exception is the opacification of the lens known as cataract. While three primary tissues have received considerable attention (the cornea, the lens, and the retina), it is important to recognize that a failure in systems other than the refractory media and the photosensitive tissues can result in the ultimate loss of ocular function. Damage to adnexal secretory tissues can affect the tear- film, which ultimately could cause the cornea to keratinise and opacify.

### 1.5.2.2 Inflammatory and cell-killing effects

#### Lens

About 90 percent of all individuals over 65 years of age have some sort of opacity in the lens, although visual acuity may not be affected sufficiently to cause visual impairment and require surgical intervention. A cataract is considered to be a loss of transparency of the lens, but only one that affects visual acuity is considered clinically significant.

It is reasonably certain that everyone, if sufficiently long-lived, will develop compromised lens transparency. At least 50 percent, and perhaps as many as 75 percent, of these opacities are associated with cortical changes, i.e., changes associated with the superficial substance of the lens. The remainder are nuclear, i.e., they represent changes in the deeper portions of the lens. The latter cataracts are due to changes in the protein and/or deep membrane systems in the lens and are for the most part reflecting photochemical effects. The cortical changes, however, are frequently associated with an altered cellular morphology and may be due to an interference in the continued normal growth and differentiation of the tissue. Such changes can occur from an accumulated exposure to various physical agents such as ionizing and non ionizing radiation.

The unique biology of the lens is the basis for its predominant pathology, i.e., cataract. The sole function of the lens is to refract incoming light onto the retina. A failure in organization and/or metabolism results in opacification. As the lens grows throughout life, there is considerable opportunity for errors in growth and differentiation. These errors are compounded by the confinement of the cells within the limiting capsule. Also, as the lens depends on a rather extensive system of cellular communication, a failure in the cortex or the most superficial regions in the lens can cause the entire tissue to fail eventually. This is likely to be the basis of the eventual complete opacification of the lens by a number of physical agents (including ionizing radiation), which have a primary effect in the lens epithelium.

Utilizing data on the development of cataracts in radiotherapy, it has been determined that an exposure of 0.15 Gy/yr to the eye should be the maximum occupational exposure, assuming a 30-year work exposure. Historically, the response of the lens to radiation has been thought to be inflammatory and cell-killing effects-related to dose with a threshold. For single doses, work suggests a 2 Gy threshold for

cataract, with 5 Gy being necessary to produce a progressive disease. However, recent work suggests that there is evidence that lens opacification, without loss of vision, can result from exposure to doses as low as 0.2 Gy.

### **1.5.3 Radiopathology–reproductive organs**

In general, the gonads are very radiosensitive. The testes contain both radiosensitive (e.g., spermatogonia) and radioresistant (e.g., mature spermatozoa) cell populations. The primary effect of radiation on the male reproductive system is temporary or permanent sterility after acute doses of approximately 2.5 Gy (250 rad) or 5 Gy (500 rad), respectively. Temporary sterility has been reported after doses as low as 150 mGy (15 rad). Reduced fertility due to decreased sperm count and motility can also be seen after chronic exposures of 20 to 50 mGy/wk (2 to 5 rad/wk) when the total dose exceeds 2.5 Gy (250 rad). These effects are not of concern with diagnostic examinations, because doses exceeding 100 mGy (10 rad) are extremely unlikely.

The ova within ovarian follicles (classified according to their size as small, intermediate, or large) are sensitive to radiation. The intermediate follicles are the most radiosensitive, followed by the large (mature) follicles and the small follicles, which are the most radioresistant. Therefore, after a radiation dose as low as 1.5 Gy (150 rad), fertility may be temporarily preserved owing to the relative radioresistance of the mature follicles, and this may be followed by a period of reduced fertility. Fertility will recur provided the exposure was not high enough to destroy the relatively radioresistant small primordial follicles. Doses in excess of 6 Gy (600 rad) are typically required to produce permanent sterility; however, sterility has been reported after doses as low as 3.2 Gy (320 rad). In either case it seems that higher doses are required to produce sterility in younger woman. Another major concern is the induction of genetic mutations and their effect on future generations.

### **1.5.4 Malignancy**

Skin cancers that might be directly attributable to interventional neuroradiological procedures have not been specifically documented, but melanoma is thought not to be related to ionizing radiation exposures. However, there are well-documented case reports of basal cell and squamous cell cancers that are attributed to radiographic and radiotherapy exposure.

The stochastic effects of radiation exposure in ocular tissues are not well known. While in the case of the lid-skin there is no reason to expect the response to differ from that of skin elsewhere, the evidence for radiogenically induced neoplastic disease in the eye is relatively sparse. The probability of radiation carcinogenesis in the ocular tissues is extremely low and the overwhelming concern for ocular morbidity should focus on inflammatory and cell-killing effect changes in the adnexal skin and cataractogenicity.

Protection of the thyroid is of concern to most interventional radiologists. However, there is little proven risk for persons exposed over the age of 20 years.

There is also an increased probability of a future malignancy in other organs that are irradiated, especially the breast, thyroid, and bone marrow, and particularly in children.

## **1.6 Thermoluminescence dosimetry**

### **1.6.1 Basic principle**

TLD relies on the fact that in certain materials electrons, where the material is irradiated, some of the electrons in the valence band (ground state) receive sufficient energy to be raised to the conduction band (metastable state), where it migrates to an electron trap. By heating the material, these metastable electrons may be given sufficient energy to escape from their unstable state and, in reverting to the valence band (ground state), they emit an optical photon (20,21). The optical photons are detected by a photomultiplier and the light output can be measured. Dosimeters can be re-used once they have been subjected to a process of annealing to eliminate any residual thermoluminescent signal (21).

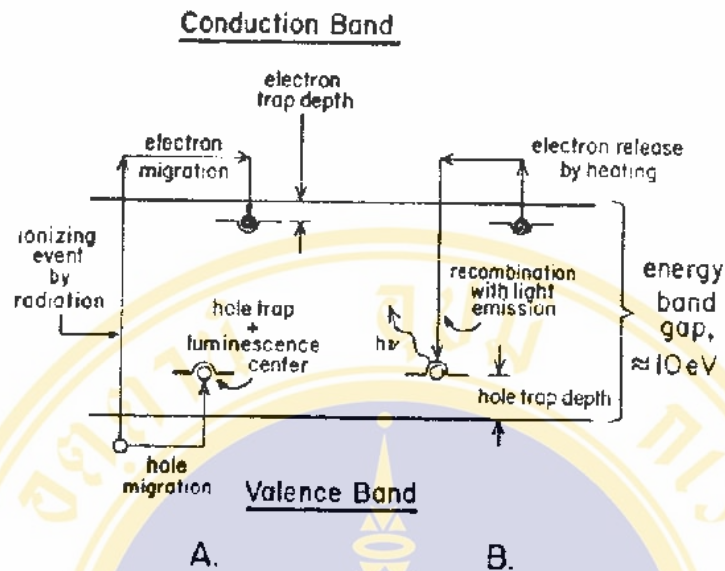


Figure 1.2 Energy-level diagram of the thermoluminescence process : (A) ionization by radiation, and trapping of electrons and holes; (B) heating to release electrons, allowing luminescence production.

### 1.6.2 Read-out

In the read-out process, by heating the thermoluminescent material after irradiated these metastable electron may be given sufficient energy to escape from their unstable and inverting to a stable state, then they emit an optical photon. The light output of the dosimeter is measured with a photomultiplier. As the temperature of the dosimeter is increased, the light output will vary. The area under the curve, i.e. the total light output, is proportional to dose. The reading may be modified in two ways (22).

1. The voltage applied to the photomultiplier can be altered. An increased voltage produces a larger signal and better resolution, but this may saturate the system.
2. A multiplication factor can be applied to the result in order to convert the reading to dose.

### 1.6.3 Annealing procedures

For each thermoluminescent material used in dosimetric applications, it is extremely important to know the procedure for restoring its basic conditions after an

irradiation. This procedure is called annealing and has two aims: the first is to empty the traps of the phosphor completely after the irradiation and read-out cycle; the second is to stabilize the electron traps in order to obtain, within narrow limits, the same glow curve even after repeated irradiations and thermal treatments (22).

#### 1.6.4 Choice of TLD material

TLD materials come in many physical and chemical forms. The most commonly used material in diagnostic radiology is lithium fluoride doped with traces of magnesium and titanium (LiF: Mg,Ti). This material is available as TLD 100 containing lithium with natural abundance (i.e. 92.5% lithium-7), TLD 600, which contains 95.6% lithium-6, and TLD 700, which is almost pure lithium-7.  $^6\text{LiF}$  is sensitive to thermal neutrons and  $^7\text{LiF}$  is not, so a combination of the two can be used for differential detection of neutrons. For routine photon dosimetry, TLD 100 is satisfactory. Many other thermoluminescent materials have been used, but for most medical uses the only others of interest are calcium Fluoride ( $\text{CaF}_2$ ), calcium sulphate ( $\text{CaSO}_4$ ), and lithium borate ( $\text{LiBO}_4$ ).  $\text{CaSO}_4$  and  $\text{CaF}_2$  are more sensitive than LiF: Mg,Ti and can be used for measuring very low doses, and have an effective atomic number of 15.6 and 16.6 respectively, which are far from 7.4 of tissue-equivalent (63,64).  $\text{LiBO}_4$  has an effective atomic number that is very close to that of tissue, so that its sensitivity increases by only 3% at low photon energies, compared to about 30% for LiF: Mg,Ti. Its drawback is that it is deliquescent (absorbs moisture) and very sensitive to ultraviolet radiation, and is consequently difficult to use. A newer material, lithium fluoride doped with about 2% of phosphorus and traces of magnesium and copper (LiF: Mg,Cu,P or TLD-100H), may supplant these other materials. The TLD-100H dosimeter is made from a nearly tissue-equivalent material with an effective atomic number of 8.2, apparently being a better option for dose measurements. The detection range of the TLD-100H dosimeter is 1  $\mu\text{Gy}$  to 10 Gy. It is up to 30 times more sensitive than LiF: Mg,Ti, and almost flat energy response, low fading rate, linear dose response, good stability at ambient temperatures and shorter annealing procedures (annealing at 240°C for 10 min). The disadvantage of LiF: Mg,Cu,P as a TLD material is that the sensitivity may be decreased by annealing at temperature over 270°C. Thus if this material is used under conditions in which the readout and annealing temperature are not strictly controlled, sensitivity may be lost.

Table 1.4 gives a summary of the properties of these materials. The discussion that follows is based on the properties of LiF: Mg,Ti, but the principles apply to any thermoluminescent dosimeter (23,24).

Table 1.4 Properties of TL dosimeters commonly used in medicine

	Lithium Fluoride	Lithium Fluoride	Lithium Borate	Calcium Sulphate	Calcium Fluoride
Most common doping material	Mg,Ti	Mg,Cu,P	Mn	Dy	Dy
Effective atomic number (tissue 7.4)	8.14	8.2	7.4	15.6	16.6
Density	2.64	2.64	2.3	2.61	3.18
Stopping power (ratio to water)					
At 100 keV	0.808	0.808	0.865	-	0.781
At 10 MeV	0.809	0.809	0.849	-	0.831
Mass energy absorption coefficient ratio					
At 100 keV	0.875	0.875	0.865	-	0.875
At 10 MeV	0.859	0.859	0.883	-	1.100
Temperature(°C) of dosimetry peak	190,210	230	200	220	200,240
Other peaks(°C)	70,130,170, 235, 260	140,190, 270	50,90	65,105,250	120,140
Wavelength (nm)	400	380	600	478,571	460,483, 576
Fading in month (approx.)	<1%	Negligible	5%	1%	13%
Annealing cycle	1h at400°C 16h at80°C	10 min at 240°C	30 min at 300°C	1h at500°C	1h at 600°C
Sensitivity relative to LiF:Mg,Ti	1	~30	0.15	20	30
Linear up to	1 Gy	10 Gy	1 Gy	30 Gy	10 Gy
Minimum measurable dose	100 µGy	1 µGy	1000µGy	1 µGy	10 µGy
Maximum dose	10 Gy	10 Gy	100 Gy	10 Gy	100Gy

### 1.6.5 Characteristic of TLD-100H

#### a) TL glow curve

The glow curve typical of LiF:Mg,Cu,P is shown in figure 1.2. The main peak is position above 200°C, preceded by a few minor peaks. Peak 4 is the main dosimetry peak, above the main peak 4 a high-temperature “tail” is observed, which is difficult to resolve into separate peaks (25).

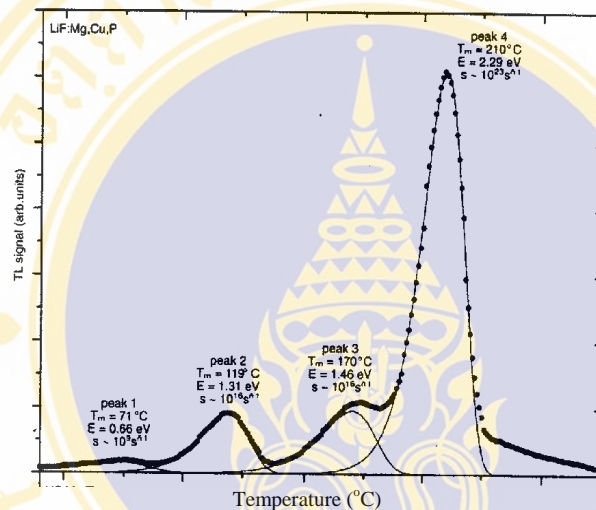


Figure 1.3 Glow curve of LiF: Mg,Cu,P detectors (pre-irradiation annealed at 240 °C for 10 minutes, heating rate 2°C.s<sup>-1</sup>, D = 1.5 mGy) (25).

#### b) Emission spectra

The TL emission occurs at a wavelength of approximately 380 nm shown in figure 1.3 (26). The light of LiF: Mg,Cu,P is violet (25). This spectrum is well matched to standard photomultiplier tubes used for TL readers.

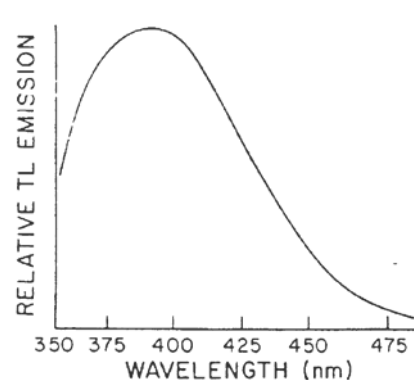


Figure 1.4 The relative TL emission spectra of LiF: Mg,Cu,P (26).

**c) Linearity**

The response of LiF: Mg,Cu,P is linear up to about 10 Gy, after which its response becomes sublinear, the TL response decreases with the dose. (21).

**d) Fading**

Fading is the term applied to decrease in the thermoluminescent signal between irradiation and read-out. As is well known, the unintentional loss of the latent information is called fading. Temperature is normally responsible for this loss, but other quantities such as light can greatly influence the latent information in the thermoluminescent material. This is caused by electrons in the lower energy traps moving into the stable state (22). For LiF: Mg,Cu,P, it is no significant signal fading was found when stored at room temperature for 1 month (21). Wu et al (23) found about 5% fading when the phosphor was stored at room temperature for 2 months.

**e) Annealing**

The residual signal after the dosimeter has been read out is removed by heating the dosimeter to a temperature above the read-out temperature. The annealing process not only removes residual signal, but also sets the sensitivity of the dosimeter (21).

Annealing process at 240°C for 10 min with LiF: Mg,Cu,P (21). It is important that the annealing temperature dose not go above 240°C, as its sensitivity and energy independence will be reduced (22).

## CHAPTER II

### OBJECTIVE

The assessment of patient doses which were studied in this project was measured in 30 patients using high sensitivity LiF:Mg,Cu,P (TLD-100H) thermoluminescent dosimeters. The aims of this study are comprised of the following.

- To determine the entrance skin doses and exit doses in the patients that occur during endovascular embolization of the arteriovenous vascular malformations which predict the possibility of inducing the deterministic effects.
- To convert the entrance skin doses to effective doses which provide an estimate of the stochastic radiation risk to the patient.
- To evaluate the technical factors which affect the patient doses.

## CHAPTER III

### LITERATURE REVIEW

Berthelsen B, Cederblad A (4) reported in a study of 5 patients during embolization of the AVMs procedures that using TLDs to measure the absorbed doses in different points of the skin of patients. A maximum patient's right eye dose of 139 mGy and a maximum thyroid dose of 10 mGy.

Theodorakou C and Horrocks JA (27) studied the irradiated areas and doses received by 30 patients during cerebral embolization. The ESD was measured by means of TLDs. They found that the average ESD was 0.77 Gy and 0.78 Gy for posteroanterior plane and lateral plane respectively. The patient's average right eye dose was 60 mGy and the average dose to the thyroid gland was 24 mGy. Seven patients received a dose above 1 Gy, one patient exceeded the threshold for transient erythema and one exceeded the threshold for temporary epilation.

Mooney RB, McKinstry CS and Kamel HAM (28) studied of absorbed dose to skin of three patients underwent intracranial arteriovenous malformations by estimated from the patient dose measurement of the Gugliemi detachable coil (GDC) embolizations patients. Skin dose was measured using TLD-100H. Several TLDs were used to measure absorbed skin dose at various points on each patient's skull. The working positions during the procedure were posteroanterior and left lateral. The maximum skin dose for three patients was 4-6 Gy, 5-7 Gy and 3-4 Gy respectively and the maximum dose to the eye was 70 mGy. The dose measurements in their study showed that the skin dose could induce deterministic effects such as temporary epilation and erythema as well as two studies above.

Thomas J. O' Dea, Richard AG and Russell RE (29) calculated entrance skin dose on 522 interventional neurological radiology procedures using an automated dosimetry system. Roshan SL, Raghuram L, Ipeson PK and Raj DV (30) evaluated radiation risk to 39 patients during cerebral interventions using DAP meter (Diamentor PTW Freiburg ,Germany) with various fluoroscopic pulse modes (3 , 15 and 30 pulse

s<sup>-1</sup>) and fluoroscopy tube potential varied between 60 kV , 62 kV and 74 kV. Both studies can conclude that the largest contribution to the patient dose is radiographic mode. Thus, monitoring fluoroscopic time alone underestimates the potential for skin injury.



## CHAPTER IV

### MATERIALS AND METHODS

#### 4.1 Materials

##### 4.1.1 Interventional neuroradiologic imaging

This work was carried out at the department of radiology, Ramathibodi hospital. The x-ray imaging system used in this study was a multidirectional biplane, TOSHIBA Infinix VB-i digital fluorography system configured to perform interventional neuroradiologic procedures (figure 4.1). Radiographic acquisitions were performed using digital subtraction angiography (DSA) where a mask frame obtained prior to the administration of iodinated contrast was subtracted digitally from subsequent images of the vasculature containing iodinated contrast. For radiographic acquisition, the frame rate ranged between 1 and 3 frame per second. In diagnostic procedures, the acquisition of radiographic images was done in biplane mode almost exclusively. In therapeutic procedures, both biplane and single plane imaging, either frontal or lateral were used during different stages of the evaluation of the embolization progress. The digital fluorography system's real-time image display function realizes biplane fluoroscopy and biplane DSA with 1024 matrixes and up to 20 frame per second (fps) acquisition for fluoro dose reduction in long interventions and 50 fps for sub-millimeter 3D angiography, display of moving roadmapping images and real-time fluoroscopic zoom, in addition to playback with up to 5X zoom and image data analysis.

#### 4.1.2 Thermoluminescence dosimetry system

Thermoluminescence dosimeters (TLDs) were used for the dose determination in Rando phantom. The thermoluminescent (TL) material used in this experiment was Lithium fluoride doped with about 2% of phosphorus and traces of magnesium and copper (LiF:Mg,Cu,P) known as TLD-100H (figure4.3). The TLDs were supplied by Bicorn RMP, that is formed into rods 1 mm in diameter and 6 mm long. They have a nominal density of  $2.64 \text{ g/cm}^3$  and an effective atomic number of 8.2, close to tissue (7.4). All TLDs were annealed by annealing oven manufactured by Harshaw Bicon, Solon Ohio, USA (figure4.4) for 10 min at  $240^\circ\text{C}$  and then cooled down to room temperature. After each procedure, the TLDs were then read-out on a Harshaw TLD reader model 5500 (Thermo RMP, Solon, OH), with background TLD measurements being deducted (figure4.5). The reader is capable of reading 50 dosimeter per loading for TL chips, rods, and cubes in a variety of sizes. The TL reader includes both the reader and a DOS-based IBM-compatible computer connected through a standard RS-232-C serial communication port. Most of the controlling features are implemented on the TLD shell software running on the PC. The reader used hot nitrogen gas heating with a closed loop feedback system to produces linearly ramped temperature accurate within  $\pm 1^\circ\text{C}$  to  $400^\circ\text{C}$  and routed through the PMT chamber to eliminate condensation. The reading cycle setting of the system were as follow : preheat temperature  $135^\circ\text{C}$  for 10 sec, and maximum temperature at  $240^\circ\text{C}$  for 20 sec to acquired TL signal. The heating rate was  $10^\circ\text{Cs}^{-1}$ . The sensitivity of TLD-100H was checked by calibration using the Harshaw model 2000-DI dosimeter (figure4.6). The model 2000-DI contains a strontium-90 (Sr-90) beta source with an approximate strength of 0.5 millicurie. The dosimeters, located in a 52-position disc, revolve under the source for a preset number of revolution. Nominal exposure rate is 4.55 mR/rev(January,1994).

The accurate calibration of this study is 3.61 mR/Rev. this calibration is based on the radiation calibration provided by the National Bureau of Standards, USA. The correction factor of Sr-90 from kerma to absorb dose rate is 0.95 cGy/R. Therefore, 1 revolution is 0.0343 mGy.



Figure 4.1 TOSHIBA Infinix VB-i digital fluorography system

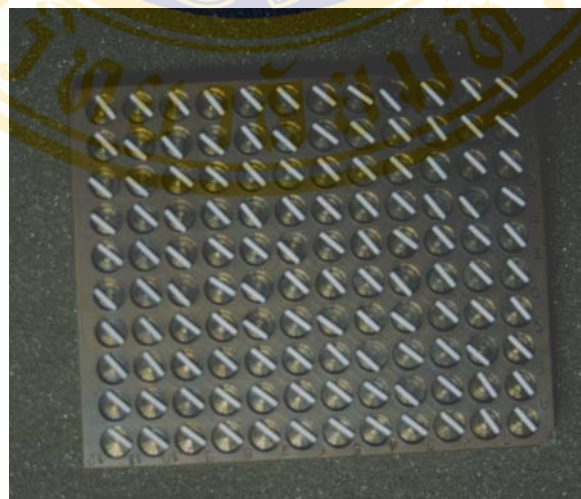


Figure 4.2 The rods of thermoluminescence dosimeter (TLD-100H).



Figure 4.3 TLD annealing oven manufactured by Harshaw Bicon, Solon Ohio, USA



Figure 4.4 Harshaw TLD reader model 5500



Figure 4.5 The Sr-90 dosimeter irradiator model 2000-DI by Harshaw nuclear system

## 4.2 Methods

This experiment was carried on into two steps :

- 4.2.1 TLD calibration
- 4.2.2 Assessment of skin dose in the patients

### 4.2.1 TLD calibration

A total of 295 TLD-100H dosimeters were used at the calibration stage.

#### 4.2.1.1 Determination of minimum detectable dose

The minimum detectable dose of TLDs were determined by reading out the residual signal (unexposed) of all TLDs in 3 times. Time and temperature profile for read out cycle were setting at preheat temperature of 135 °C for 10 second and maximum temperature at 240 °C for 20 second to acquire TL signal. The heating rate was 10 °C per second. The minimum detectable dose of TLDs were calculated as the three times of standard deviation (3 SD) (82).

#### 4.2.1.2 Grouping and determination of the correction factor for sensitivity of each group

1. All TLDs were annealed in the dedicated TLD annealing oven for 10 min at 240°C and were exposed to a known dose of 30 revolution (~1 mGy) from a Sr-90 calibration source
2. Read the TLDs, record the signals and repeat twice.
3. Set twelve of recorded signals in a group.
4. The correction factor (CF) for sensitivity of each group was calculated by ;

$$\text{Correction factor (CF) for sensitivity} = X / X_i$$

Where X is average reading for all TLDs

$X_i$  is average reading for 12 TLDs of the group i

#### 4.2.1.3 Calibration for absolute measurement

In this study all TLDs were calibrated by using Sr-90 from the Harshaw model 2000-DI Per our current are due to dosimeter.

1. Select the 8 TLDs from each group, then expose them with known dose in the M2000DI instrument for 1, 5, 10, 50, 100, 500, 1000, 3000 Revolutions.
2. Read the TLDs and record.
3. The reading of exposed TL signals were averaged for each group and converted to absorbed dose
4. The TL response (nC) were plotted against the dose (mGy).

#### **4.2.2 Patient dose measurements**

Measurements were made on 30 patients that underwent embolization of AVMs. The absorbed dose at various points on the skin of the patient was determined using TLDs. Single TLD encapsulated in plastic tube were taped to the skin of the patients in the assumed entrance area of the x-ray beam on the back of the head, thyroid gland, breast, abdomen and gonad (posteroanterior plane) as well as the right side of the head, thyroid gland, breast, abdomen and gonad (lateral plane). TLDs were also placed in the left lateral head, thyroid gland, breast, abdomen and gonad (lateral plane) and on the head, thyroid gland, breast, abdomen and gonad (anteroposterior plane) that assumed exit area of the x-ray beam. Care was always taken to ensure that the TLDs were positioned at exactly the same locations on every patient. The embolization procedures were performed by using standard techniques. The tube setting were controlled by the automatic exposure control (AEC).

#### **4.2.3 Data recorded during each procedure**

During each procedure the entrance skin dose and exit dose for fluoroscopy and radiography mode and for both planes, the patient data and the technical parameters such as the tube voltage, the tube current, exposure time, frame rate, and number of images were recorded.

#### **4.2.4 Data analysis**

In this study, values of entrance skin dose, exit dose and effective dose were determined for each procedure. The analysis included influence of technical factors to patient doses. In addition, an investigation regarding the importance of fluoroscopy relative to radiographic image acquisitions, as well as the relative importance of the frontal versus the lateral imaging projection plane. Patient doses were quantified to investigate how patient skin doses compare with the threshold for the induction of deterministic effects.

## CHAPTER V

### RESULTS AND DISCUSSION

#### 5.1 TLD calibration

##### 5.1.1 The correction factor for sensitivity of each group

The standard deviation (SD) of residual signal of the batch of TLDs is 0.004 nC. Therefore, the detection threshold calculated by three times of standard deviation (3SD) is equal to 0.013 nC and the %CV is  $\pm 5.3$ .

The correction factor (CF) for sensitivity of each group shown in table 5.1.

##### 5.1.2 The absolute dose calibration

The conversion factor for exposure dose to absorbed dose is 0.95 cGy/R and 1 revolution of Sr-90 irradiator is 3.61 mR. Therefore, 1 revolution of Sr-90 irradiator is equal to 0.0343 mGy and then the known dose in mGy are 0.034, 0.172, 0.343, 1.715, 3.430, 34.30 and 102.90 respectively.

The TL response (nC) were plotted against the dose (mGy) for 0.034 mGy to 3.43 mGy and 3.43 mGy to 102.9 mGy respectively, the curve shown in figure 5.1 and 5.2. The linear relationships can be found as shown also by the linear equations with excellent  $R^2$ .

The equation are  $Y = 0.1272X - 0.0177$  for the dose of 0.034 mGy to 3.43 mGy and  $Y = 0.1441X - 0.5891$  for the dose of 3.43 mGy to 102.90 mGy where Y is the absorbed dose in mGy and X is the TL response in nC.

Table 5.1 Correction Factor (CF) for sensitivity of each groups of TLD

Group	Signal (nC)												Mean ± SD	CF
	1	2	3	4	5	6	7	8	9	10	11	12		
<b>1A</b>	3.38	3.53	3.63	3.83	3.89	4.15	4.18	4.24	4.25	4.26	4.26	4.30	<b>3.99±0.33</b>	<b>1.423</b>
<b>1B</b>	4.30	4.32	4.36	4.36	4.36	4.37	4.40	4.43	4.43	4.44	4.44	4.47	<b>4.36±0.05</b>	<b>1.294</b>
<b>1C</b>	4.49	4.55	4.56	4.58	4.62	4.62	4.63	4.64	4.67	4.69	4.69	4.74	<b>4.62±0.07</b>	<b>1.228</b>
<b>1D</b>	4.75	4.76	4.81	4.83	4.85	4.85	4.86	4.89	4.90	4.92	4.92	4.93	<b>4.85±0.06</b>	<b>1.170</b>
<b>1E</b>	4.93	4.95	4.95	4.96	4.97	4.99	5.00	5.00	5.02	5.02	5.03	5.03	<b>4.99±0.03</b>	<b>1.139</b>
<b>1F</b>	5.04	5.05	5.05	5.10	5.11	5.12	5.16	5.17	5.17	5.17	5.20	5.20	<b>5.13±0.06</b>	<b>1.107</b>
<b>1G</b>	5.22	5.23	5.23	5.23	5.27	5.28	5.29	5.29	5.30	5.33	5.33	5.34	<b>5.28±0.06</b>	<b>1.076</b>
<b>1H</b>	5.34	5.37	5.37	5.38	5.38	5.39	5.40	5.41	5.42	5.43	5.43	5.45	<b>5.40±0.04</b>	<b>1.052</b>
<b>1I</b>	5.45	5.46	5.46	5.47	5.47	5.48	5.48	5.49	5.51	5.52	5.53	5.53	<b>5.49±0.03</b>	<b>1.035</b>
<b>1J</b>	5.54	5.54	5.54	5.55	5.55	5.57	5.58	5.63	5.63	5.64	5.67	5.70	<b>5.60±0.03</b>	<b>1.015</b>
<b>2A</b>	5.72	5.72	5.73	5.73	5.74	5.75	5.75	5.77	5.77	5.78	5.80	5.82	<b>5.76±0.06</b>	<b>0.987</b>
<b>2B</b>	5.83	5.89	5.89	5.89	5.90	5.91	5.92	5.94	5.94	5.94	5.94	5.95	<b>5.91±0.03</b>	<b>0.961</b>
<b>2C</b>	5.96	5.96	5.97	5.99	6.01	6.04	6.06	6.07	6.12	6.12	6.16	6.18	<b>6.05±0.03</b>	<b>0.938</b>
<b>2D</b>	6.19	6.20	6.21	6.22	6.23	6.24	6.24	6.30	6.33	6.33	6.34	6.34	<b>6.26±0.08</b>	<b>0.907</b>
<b>2E</b>	6.38	6.45	6.47	6.47	6.49	6.51	6.52	6.55	6.55	6.55	6.57	6.60	<b>6.51±0.06</b>	<b>0.873</b>
<b>2F</b>	6.61	6.62	6.65	6.67	6.70	6.70	6.71	6.72	6.74	6.74	6.82	6.83	<b>6.71±0.06</b>	<b>0.847</b>
<b>2G</b>	6.92	6.95	6.96	6.98	7.01	7.05	7.05	7.09	7.10	7.19	7.21	7.21	<b>7.06±0.07</b>	<b>0.805</b>
<b>2H</b>	7.25	7.27	7.27	7.29	7.30	7.34	7.35	7.39	7.40	7.40	7.52	7.58	<b>7.36±0.1</b>	<b>0.771</b>
<b>2I</b>	7.64	7.72	7.76	7.77	7.77	7.95	-	-	-	-	-	-	<b>7.77±0.1</b>	<b>0.750</b>

Mean reading for all TLDs = 5.69

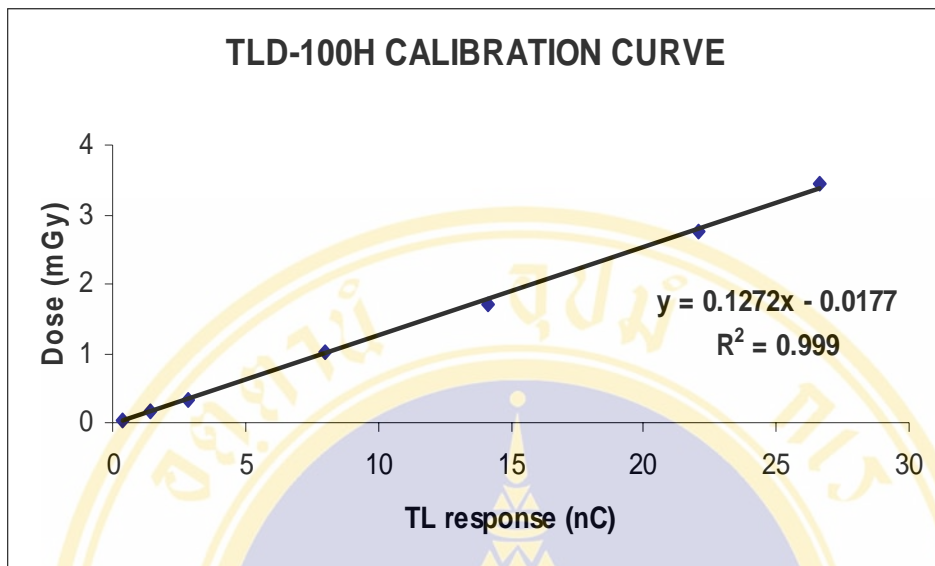


Figure 5.1 The calibration curve of TL signals for absorbed doses of 0.034 mGy to 3.43 mGy.

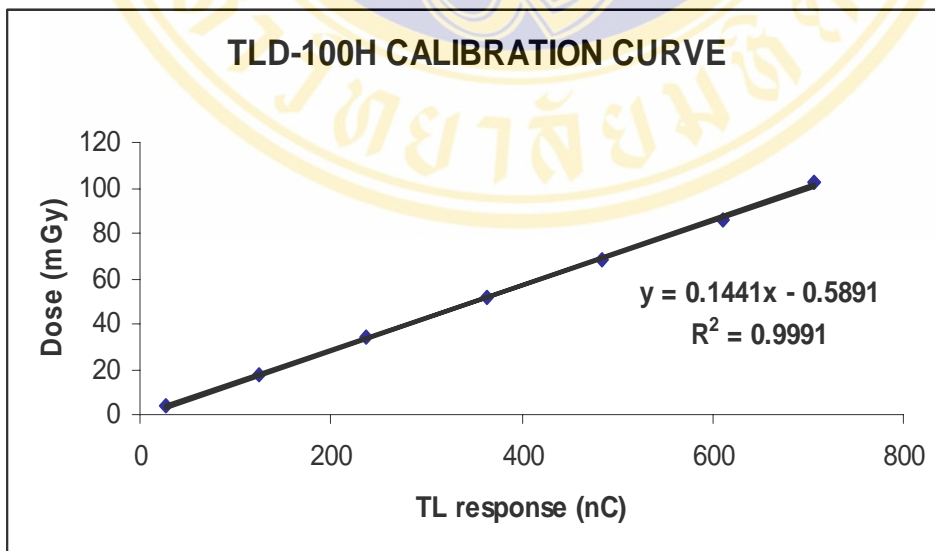


Figure 5.2 The calibration curve of TL signals for absorbed doses of 3.43 mGy to 102.90 mGy.

## 5.2 Patient doses

Dose assessment performed in 30 patients, 17 ( 8 male patients and 9 female patients ) underwent the first endovascular embolization of AVMs and 13 ( 8 male patients and 5 female patients ) underwent the second endovascular embolization of AVMs. The mean age was 35.5 year ( range from 13 to 63 years ). The different technique for endovascular embolization of AVMs procedures are summarized in table 5.2. This table represents technical parameters for fluoroscopy and radiography. Also sex, age, weight, thickness, field of view and total procedure time are presented. An overview, there is no major different in kV and mA setting between each patients for fluoroscopy and radiography.

### 5.2.1 Entrance skin dose and exit dose

Table 5.3 represents the entrance skin dose and exit dose of eye, thyroid, breast, abdomen and gonad for frontal plane and lateral plane. The maximum, median and minimum entrance skin dose of each organ for frontal plane and lateral plane are shown in figure 5.3 and 5.4, respectively. The maximum, median and minimum exit dose of each organ for frontal plane and lateral plane are shown in figure 5.5 and 5.6, respectively. These values show a wide distribution of the entrance skin dose and exit dose among patients.

The highest doses for the endovascular embolization of AVMs procedure are delivered to the eye region. This location is closest to the area under examination and to the lateral x-ray tube. Other areas more distant from the beam have doses lower. It is important to mention that in those region is the radiosensitive organ. For frontal plane the entrance skin dose of eye was within the range of 40.20 mGy to 1310.05 mGy and 1.54 mGy to 170 mGy for lateral plane. The median values were 805.22 mGy and 110.72 mGy for frontal and lateral plane, respectively. The exit dose of eye has the median value of 110.72 mGy (range from 1.54 mGy to 170 mGy) for frontal plane and 4.6 mGy (range from 0.12 mGy to 40.85 mGy) for lateral plane. The range for exit dose is very small compared to the entrance skin dose. For all other organs in table 5.3 and figure 5.3 to 5.6, the median doses are substantially lower.

The entrance skin doses of the eye measured in this study may be compared to the data available in the literature. Berthelsen et al (4) reported the maximum patient's right eye dose of 139 mGy. Theodorakou et al (27) reported the patient's average right eye dose was 60 mGy. Whereas Mooney et al (28) reported the maximum dose to the eye was 70 mGy. Detail comparison with these studies was problematic due to differences in clinical cases and setting imaging protocols and radiographic equipment. Nevertheless, eye dose in this study appear higher which is likely a result of use of more complicated protocols.

With the biplane system used in this study, the doses at the back and right side of the body were much higher than at the front or left side. An explanation for this can be found in the position of the x-ray tubes that is under the patient tabletop for the frontal tube and at the patient's right side for the lateral tube.

The entrance skin doses for the frontal plane were found to be slightly higher than for the lateral plane and that was expected since the number of images and the fluoroscopy time for frontal plane were higher than those for the lateral plane.

For both planes most of the doses are below 2 Gy threshold level for early transient erythema. Two patients have received the entrance skin dose of eye above 1 Gy. The maximum values of 1.31 Gy for eye could be considered as significant. Although, it is still far below the threshold dose of cataract ( 5 Gy ) but near the threshold dose for lens opacities of 2 Gy.

At lower doses, sign of erythema would be fleet and faint, which would make detection difficult. As observed, there were no cases of erythema in 30 patients who underwent endovascular embolization of AVMs procedure that the data shown in table 5.3. For most patients, their maximum entrance skin dose was below the threshold dose for induction of the deterministic effects. The factors which could affect the threshold doses for induction of the deterministic effects include the anatomical location, size of the irradiated region, oxygenation, patient age, genetic background and hormonal status (31).

### **5.2.2 Effective dose**

In the patients also measured the absorbed doses in points of the skin close to important organs in or near the primary radiation field. It was assumed that the

radiation doses to tissues or organs were approximately the same as those in the skin surface above.

The effective dose of eye, thyroid, breast, abdomen and gonad for frontal and lateral plane are shown in table 5.4. The maximum, median and minimum effective dose values of each organ for frontal and lateral plane are shown in figure 5.7 and 5.8, respectively. The eye region received the highest effective dose. For frontal plane the effective dose of the eye was within the range 2.01- 65.5 mSv with the median value of 40.26 mSv while for lateral plane the effective dose was within the range 0.08 - 8.5 mSv with the median value of 5.54 mSv.

The median effective dose of the eye for the endovascular embolization of AVMs procedures may be compared to effective dose for other common radiologic examinations that also use ionizing radiation. Effective doses for chest x-ray are of the order of 0.05 mSv, for skull radiographic examinations of the order of 0.2 mSv, for abdominal radiographic examinations between 0.5 and 1.5 mSv and for excretory urogram examinations between 2.5 and 5.0 mSv. Patients undergoing barium enemas receive doses between 3.0 and 7.0 mSv, head CT scans measure effective dose between 1 and 2 mSv, and body CT scans about 5 mSv. A routine coronary angiographic procedure measures between 3.0 and 6.0 mSv. The median effective dose of the eye for the endovascular embolization of AVMs procedures are therefore markedly higher than those normally encountered in diagnostic radiology. The median effective dose of the eye for the endovascular embolization of AVMs procedures can also be compared with natural background in the United States (3 mSv/year) (31). The natural background equivalent radiation time is approximately 13 years for frontal plane and approximately 2 years for lateral plane.

The median effective dose of 40.25 mSv for frontal plane is comparable to the risk of dying from lung cancer when smoking approximately 670 packs of cigarettes, or the risk of dying in an automobile when driving a distance of approximately 33,541 miles. While the median effective dose of 5.54 mSv for lateral plane is comparable to the risk of dying from lung cancer when smoking approximately 92 packs of cigarettes, or the risk of dying in an automobile when driving a distance of approximately 4,616 miles.

Table 5.2 Summary of the technical parameters for endovascular embolization of AVMs procedures

	Patient no.				
	1	2	3	4	5
<b>Sex/Age</b>	F/22	M/14	M/38	M/45	F/32
<b>Weight (kg)</b>	58	51	70	63	52
<b>No. of procedure</b>	1	2	2	2	1
<b>Procedure time (min)</b>	64	83	82	70	97
<b>FOV (inch)</b>	5,7,9,12	7,9,12	7,9,12	7,9,12	9
<b>Frontal</b>					
<b>SID (cm)</b>	93-104	94	93-104	94-110	97-110
<b>Thickness (cm)</b>					
Eye	14	19	20	19	16
Thyroid	11	13	13	13.5	12
Breast	33	30	37	32	30
Abdomen	27	25	33	30	24
Gonad	38	33	40	35	35
<b>Fluoroscopy mode</b>					
Fluoroscopy time (min)	12.7	19.6	25.9	8.4	11.4
kV	70	70	70	70-74	70
mAs	32-52	32-50	32-50	25-50	32-50
<b>Radiography mode</b>					
kV	74	74	74	74-88	74-88
mAs	220-300	93-240	200-400	200-400	200-400
Frame rate	3,25	3	1,3	3,25	2,3,25
No.of series	8	6	18	8	9
No.of image	200	76	226	412	224
<b>Lateral</b>					
<b>SID (cm)</b>	107-119	107-119	94	93-110	105-120
<b>Thickness (cm)</b>					
Eye	18	18	19.5	20	17.5
Thyroid	10	8	13	13	11
Breast	22	16	23.5	21	22
Abdomen	20	15	23	23	21
Gonad	20	16	22	20	22
<b>Fluoroscopy mode</b>					
Fluoroscopy time (min)	9.3	12.3	15.6	7.1	8
kV	74	74	74	74-88	74
mAs	30-52	32-60	32-50	32-60	32-50
<b>Radiography mode</b>					
kV	74	74	74	74	74
mAs	416-540	92-400	200-400	200-320	200-400
Frame rate	1,3	2,3	3	3	2,3
No.of series	8	9	8	7	7
No.of image	162	143	64	122	116

Table 5.2 Summary of the technical parameters for endovascular embolization of AVMs procedures (Continued)

	Patient no.				
	6	7	8	9	10
<b>Sex/Age</b>	M/47	M/58	M/30	M/41	F/26
<b>Weight (kg)</b>	62	54	57	60	52
<b>No. of procedure</b>	2	1	1	2	2
<b>Procedure time (min)</b>	38	85	76	42	25
<b>FOV (inch)</b>	9	12	5,9	7,9	9
<b>Frontal</b>					
<b>SID (cm)</b>	94-110	97-107	93-107	94-110	97-110
<b>Thickness (cm)</b>					
Eye	20	18	19.5	20.5	18
Thyroid	13	12	13	14	13
Breast	32	30	33	35	32
Abdomen	30	28	30	34	25
Gonad	33	30	31	32	33
<b>Fluoroscopy mode</b>					
Fluoroscopy time (min)	3.2	16.8	29.3	6.9	2.1
kV	70	70	70	70	70
mAs	32-50	32-50	32-60	32-60	32-50
<b>Radiography mode</b>					
kV	74-84	74-84	74-88	74	74
mAs	200-400	160-400	160-400	200-400	200-320
Frame rate	3,25	1,3,25	2,3,25	2,3	3
No.of series	5	22	19	5	3
No.of image	202	696	496	128	164
<b>Lateral</b>					
<b>SID (cm)</b>	104-106	112-117	104-115	104-110	104-110
<b>Thickness (cm)</b>					
Eye	22	20	20	22	18
Thyroid	12	12	13	13.5	10
Breast	25	23	25	28	22
Abdomen	23	23	27	30	20
Gonad	23	22	24	28	20
<b>Fluoroscopy mode</b>					
Fluoroscopy time (min)	1.8	4.4	10.4	5.1	1.2
kV	74	74	74	74	74
mAs	32-50	32-60	32-60	32-60	32-50
<b>Radiography mode</b>					
kV	74	74	74	74	74
mAs	200-280	230-400	200-320	200-320	200-320
Frame rate	3	3	3	2,3	3
No.of series	4	4	13	5	3
No.of image	122	72	163	82	140

Table 5.2 Summary of the technical parameters for endovascular embolization of AVMs procedures (Continued)

	Patient no.				
	11	12	13	14	15
<b>Sex/Age</b>	F/63	M/31	M/45	M/13	F/58
<b>Weight (kg)</b>	67	60	71	47	46
<b>No. of procedure</b>	1	1	1	1	2
<b>Procedure time (min)</b>	123	65	75	135	62
<b>FOV (inch)</b>	7,9,12	7,9	9	9	9
<b>Frontal</b>					
<b>SID (cm)</b>	93-110	94-107	93-110	94-106	93-109
<b>Thickness (cm)</b>					
Eye	21	18	20	15	17.5
Thyroid	13	14	15	10	12
Breast	38	30	38	30	33
Abdomen	32	29	36	28	27
Gonad	40	31	35	31	32
<b>Fluoroscopy mode</b>					
Fluoroscopy time (min)	20.8	20.3	2.7	23.1	8.2
kV	70	70	70	70	70
mAs	32-60	32-50	32-50	32-50	32-50
<b>Radiography mode</b>					
kV	70	70	70	70	70
mAs	200-500	200-400	200-400	200-400	200-400
Frame rate	3,25	3,25	3,25	3,25	3
No.of series	11	18	6	29	7
No.of image	534	450	440	926	305
<b>Lateral</b>					
<b>SID (cm)</b>	94-105	97-110	97-100	94-105	94-110
<b>Thickness (cm)</b>					
Eye	22	20	21	16	18
Thyroid	12	13	13	9.5	12
Breast	28	25	27	23.5	28
Abdomen	30	24	30	20	25
Gonad	28	22	24	21	25
<b>Fluoroscopy mode</b>					
Fluoroscopy time (min)	9.8	6.1	1.3	7.8	5.3
kV	74	74	74	74	74
mAs	32-50	32-50	32-50	32-50	32-50
<b>Radiography mode</b>					
kV	74-88	74	74	74	74
mAs	200-500	200-400	200-500	200-500	200-500
Frame rate	3	3	3	3	3
No.of series	9	15	4	24	7
No.of image	247	136	162	341	189

Table 5.2 Summary of the technical parameters for endovascular embolization of AVMs procedures (Continued)

	<b>Patient no.</b>				
	16	17	18	19	20
<b>Sex/Age</b>	M/29	F/56	M/44	F/35	F/50
<b>Weight (kg)</b>	65	63	61	50	58
<b>No. of procedure</b>	2	2	1	2	1
<b>Procedure time (min)</b>	50	30	58	75	135
<b>FOV (inch)</b>	7,9	9	7,9	7,9	5,7,9,12
<b>Frontal</b>					
<b>SID (cm)</b>	94-107	94-110	94-107	94-110	94-110
<b>Thickness (cm)</b>					
Eye	20	19	19.5	15	16
Thyroid	13	12.5	12.5	12	13.5
Breast	35	33	35	31	35
Abdomen	38	32	37	29	33
Gonad	36	34	37	34	38
<b>Fluoroscopy mode</b>					
Fluoroscopy time (min)	3.1	1.6	1.3	6.4	24.7
kV	70	70	70	70	70
mAs	32-60	32-50	32-50	32-50	32-50
<b>Radiography mode</b>					
kV	70-88	70	70	70	70-84
mAs	200-500	200-500	200-500	200-400	200-500
Frame rate	3,25	3	3,25	3	2,3,25
No.of series	5	3	5	3	13
No.of image	312	86	490	72	748
<b>Lateral</b>					
<b>SID (cm)</b>	103-107	97-110	94-110	97-110	97-110
<b>Thickness (cm)</b>					
Eye	17	15	18	16	16
Thyroid	14	12	13	12	13
Breast	23	24	23	20	26
Abdomen	29	25	25	17	25
Gonad	25	26	24	20	25
<b>Fluoroscopy mode</b>					
Fluoroscopy time (min)	0.9	0.7	0.6	4.5	6.9
kV	74	74	74	74	74
mAs	32-50	32-50	32-50	32-50	32-50
<b>Radiography mode</b>					
kV	74	74	74	74	74
mAs	200-400	200-400	200-500	200-400	200-400
Frame rate	3	3	3	3	3
No.of series	3	3	4	3	9
No.of image	84	40	122	54	348

Table 5.2 Summary of the technical parameters for endovascular embolization of AVMs procedures (Continued)

	<b>Patient no.</b>				
	26	27	28	29	30
<b>Sex/Age</b>	F/33	M/40	M/28	F/27	F/18
<b>Weight (kg)</b>	53	57	62	52	48
<b>No. of procedure</b>	1	1	1	2	1
<b>Procedure time (min)</b>	62	78	93	68	74
<b>FOV (inch)</b>	7,9,12	7,9,12	5,7,9,12	7,9,12	7,9,12
<i>Frontal</i>					
<b>SID (cm)</b>	93-104	94-104	93-103	94-105	93-110
<b>Thickness (cm)</b>					
Eye	14	18	16.5	16	16
Thyroid	13	14.5	13	13	12.5
Breast	34	32	32	32	32
Abdomen	27	26	27	26	25
Gonad	38	32	38	33	30
<b>Fluoroscopy mode</b>					
Fluoroscopy time (min)	10.4	13.6	20.5	16.8	12.1
kV	70	70	70	70	70
mAs	32-52	32-50	32-52	32-50	32-50
<b>Radiography mode</b>					
kV	74	74	74	74	74
mAs	220-300	200-400	220-300	93-240	200-400
Frame rate	3,25	3	3,25	3	3,25
No.of series	9	6	12	5	11
No.of image	182	102	234	62	194
<i>Lateral</i>					
<b>SID (cm)</b>	97-110	105-110	94-110	97-110	103-110
<b>Thickness (cm)</b>					
Eye	16	19.5	17	16	16
Thyroid	13	12.5	12.5	12.5	13
Breast	25	24	23	22	23
Abdomen	21	22	20	21	25
Gonad	22	23	20	25	26
<b>Fluoroscopy mode</b>					
Fluoroscopy time (min)	8.6	5.9	12.7	10.3	9.5
kV	74	74	74	74	74
mAs	30-52	32-50	30-50	32-50	32-50
<b>Radiography mode</b>					
kV	74	74	74	74	74
mAs	200-400	200-400	200-400	200-400	200-400
Frame rate	3	3	1,3	2,3	3
No.of series	8	5	10	10	8
No.of image	138	92	202	126	120

Table 5.3 The entrance skin dose and exit dose

	Patient no.				
	1	2	3	4	5
<b>Frontal</b>					
<i>Entrance skin dose (mGy)</i>					
Rt. eye	704.57	109.93	235.45	899.13	712.64
Lt. eye	233.95	39.32	217.34	610.56	256.15
Thyroid	91.31	47.28	52.66	92.67	89.03
Rt. breast	3.96	1.53	18.88	4.22	3.55
Lt. breast	3.95	1.14	15.95	4.17	3.39
Abdomen	0.84	0.66	8.03	0.86	0.95
Gonad	0.62	0.47	7.18	0.66	0.71
<i>Exit dose (mGy)</i>					
Rt. eye	136.97	3.70	14.04	169.94	129.97
Lt. eye	39.35	1.35	12.42	98.16	40.40
Thyroid	11.68	21.00	2.17	11.02	12.89
Rt. breast	0.53	0.80	0.77	0.89	0.50
Lt. breast	0.46	0.59	4.67	0.42	0.42
Abdomen	0.20	0.19	0.29	0.27	0.22
Gonad	0.18	0.19	0.22	0.19	0.17
<b>Lateral</b>					
<i>Entrance skin dose (mGy)</i>					
Eye	47.01	449.67	12.55	46.46	46.13
Thyroid	50.67	76.59	3.78	43.16	41.09
Breast	2.85	1.10	3.75	2.24	2.16
Abdomen	0.94	0.64	3.07	0.72	0.62
Gonad	0.43	0.43	2.83	0.42	0.40
<i>Exit dose (mGy)</i>					
Eye	1.46	34.60	6.89	1.32	1.41
Thyroid	18.25	7.22	2.87	20.56	18.19
Breast	0.66	0.86	3.11	0.86	0.60
Abdomen	0.25	0.26	1.11	0.22	0.26
Gonad	0.20	0.24	1.61	0.21	0.22

Table 5.3 The entrance skin dose and exit dose (Continued)

	Patient no.				
	6	7	8	9	10
<b>Frontal</b>					
<i>Entrance skin dose (mGy)</i>					
Rt. eye	268.98	1024.12	796.05	52.17	40.99
Lt. eye	256.59	916.46	311.53	48.95	37.17
Thyroid	79.69	86.51	94.31	41.07	35.06
Rt. breast	2.86	4.17	5.69	1.99	1.82
Lt. breast	2.32	4.02	3.17	1.95	1.72
Abdomen	0.49	1.22	0.75	0.32	0.31
Gonad	0.37	0.86	0.61	0.21	0.19
<i>Exit dose (mGy)</i>					
Rt. eye	16.35	134.51	142.07	3.65	2.73
Lt. eye	15.28	112.70	45.71	3.15	2.42
Thyroid	5.69	45.99	15.55	1.69	1.35
Rt. breast	0.47	1.06	0.89	0.49	0.40
Lt. breast	0.45	1.05	0.44	0.42	0.34
Abdomen	0.17	0.58	0.21	0.10	0.11
Gonad	0.11	0.27	0.16	0.06	0.07
<b>Lateral</b>					
<i>Entrance skin dose (mGy)</i>					
Eye	89.65	76.57	102.69	46.36	37.16
Thyroid	36.95	28.37	48.65	39.26	31.70
Breast	0.86	0.71	2.47	1.89	1.64
Abdomen	0.22	0.20	1.03	0.65	0.49
Gonad	0.08	0.07	0.41	0.41	0.37
<i>Exit dose (mGy)</i>					
Eye	5.95	6.25	14.62	1.24	1.21
Thyroid	2.11	1.68	12.12	5.37	1.95
Breast	0.12	0.11	0.82	0.42	0.24
Abdomen	0.06	0.07	0.27	0.19	0.11
Gonad	0.01	0.01	0.20	0.16	0.08

Table 5.3 The entrance skin dose and exit dose (Continued)

	<b>Patient no.</b>				
	11	12	13	14	15
<b>Frontal</b>					
<i>Entrance skin dose (mGy)</i>					
Rt. eye	1003.56	932.47	679.33	1201.65	678.94
Lt. eye	784.90	738.22	577.22	924.57	198.59
Thyroid	76.47	62.10	43.91	132.85	85.93
Rt. breast	5.64	3.59	2.24	10.57	3.21
Lt. breast	4.31	3.10	2.04	7.22	2.91
Abdomen	1.47	1.10	1.11	1.25	0.70
Gonad	0.95	0.82	0.76	0.86	0.51
<i>Exit dose (mGy)</i>					
Rt. eye	121.04	98.80	74.44	135.68	112.35
Lt. eye	98.46	79.37	60.00	100.97	32.30
Thyroid	38.99	29.47	21.57	45.85	9.13
Rt. breast	0.99	0.79	0.56	1.14	0.42
Lt. breast	1.19	0.72	0.52	1.22	0.40
Abdomen	0.37	0.33	0.22	0.46	0.18
Gonad	0.21	0.18	0.18	0.31	0.12
<b>Lateral</b>					
<i>Entrance skin dose (mGy)</i>					
Eye	110.28	93.47	63.27	143.66	42.83
Thyroid	55.03	39.95	29.11	58.83	39.92
Breast	2.77	2.11	1.63	2.15	2.11
Abdomen	1.21	0.99	0.71	1.15	0.72
Gonad	0.43	0.33	0.23	0.38	0.34
<i>Exit dose (mGy)</i>					
Eye	13.95	10.38	7.95	20.95	1.11
Thyroid	12.38	9.99	5.00	15.55	5.95
Breast	0.77	0.53	0.37	0.89	0.59
Abdomen	0.20	0.19	0.16	0.24	0.19
Gonad	0.22	0.12	0.10	0.25	0.13

Table 5.3 The entrance skin dose and exit dose (Continued)

	Patient no.				
	16	17	18	19	20
<b>Frontal</b>					
<i>Entrance skin dose (mGy)</i>					
Rt. eye	634.15	40.20	732.98	41.79	1310.05
Lt. eye	402.64	33.90	245.96	30.56	867.86
Thyroid	64.92	16.78	93.96	15.96	100.95
Rt. breast	2.05	0.61	4.24	0.63	6.96
Lt. breast	1.70	0.56	4.18	0.55	6.21
Abdomen	0.27	0.33	0.81	0.29	1.24
Gonad	0.12	0.24	0.60	0.21	0.95
<i>Exit dose (mGy)</i>					
Rt. eye	85.96	1.94	128.50	1.54	145.86
Lt. eye	23.08	0.66	33.56	0.53	41.84
Thyroid	7.83	9.25	10.84	8.44	12.75
Rt. breast	0.42	0.33	0.42	0.32	0.55
Lt. breast	0.20	0.25	0.41	0.22	0.52
Abdomen	0.09	0.10	0.19	0.08	0.23
Gonad	0.09	0.09	0.18	0.07	0.20
<b>Lateral</b>					
<i>Entrance skin dose (mGy)</i>					
Eye	26.95	11.75	42.98	13.62	149.85
Thyroid	18.40	12.67	32.49	11.96	60.95
Breast	1.05	0.71	2.12	1.01	2.32
Abdomen	0.10	0.24	0.86	0.22	1.43
Gonad	0.10	0.11	0.37	0.10	0.34
<i>Exit dose (mGy)</i>					
Eye	0.12	0.36	1.93	0.34	19.94
Thyroid	2.44	4.56	15.27	3.86	14.86
Breast	0.17	0.17	0.79	0.13	0.85
Abdomen	0.07	0.06	0.42	0.05	0.21
Gonad	0.05	0.05	0.36	0.04	0.20

Table 5.3 The entrance skin dose and exit dose (Continued)

	<b>Patient no.</b>				
	21	22	23	24	25
<b>Frontal</b>					
<i>Entrance skin dose (mGy)</i>					
Rt. eye	177.10	371.20	305.06	1189.12	453.06
Lt. eye	70.46	192.58	38.95	798.95	165.11
Thyroid	12.84	250.94	62.02	89.56	51.34
Rt. breast	7.25	8.22	5.36	5.70	3.33
Lt. breast	7.19	7.57	4.45	5.13	3.02
Abdomen	0.74	2.72	1.63	1.01	0.83
Gonad	0.65	1.01	0.47	0.82	0.50
<i>Exit dose (mGy)</i>					
Rt. eye	27.55	30.36	15.13	156.75	137.65
Lt. eye	11.88	15.06	1.16	45.97	43.66
Thyroid	1.61	20.48	9.41	16.96	11.90
Rt. breast	1.25	3.54	1.39	0.85	0.64
Lt. breast	2.70	3.42	1.23	0.61	0.51
Abdomen	0.18	0.25	0.97	0.32	0.34
Gonad	0.28	0.19	0.33	0.25	0.25
<b>Lateral</b>					
<i>Entrance skin dose (mGy)</i>					
Eye	63.92	27.47	128.47	137.94	81.00
Thyroid	9.02	83.15	7.52	54.91	31.87
Breast	7.14	3.26	1.31	2.05	1.75
Abdomen	0.63	1.06	1.53	1.21	0.83
Gonad	0.52	0.23	0.35	0.22	0.21
<i>Exit dose (mGy)</i>					
Eye	35.54	1.47	29.06	23.87	20.48
Thyroid	3.09	33.36	4.98	17.96	15.54
Breast	2.74	0.51	0.83	1.00	0.93
Abdomen	0.19	0.42	0.56	0.28	0.32
Gonad	0.26	0.19	0.27	0.24	0.22

Table 5.3 The entrance skin dose and exit dose (Continued)

	Patient no.				
	26	27	28	29	30
<b>Frontal</b>					
<i>Entrance skin dose (mGy)</i>					
Rt. eye	641.78	184.74	721.04	92.73	385.75
Lt. eye	241.05	84.89	255.21	32.84	200.83
Thyroid	85.97	14.94	100.28	37.95	263.69
Rt. breast	3.37	8.11	4.12	1.14	8.94
Lt. breast	2.95	7.23	3.85	0.94	7.78
Abdomen	0.66	0.69	0.79	0.54	3.00
Gonad	0.49	0.58	0.59	0.42	1.21
<i>Exit dose (mGy)</i>					
Rt. eye	145.09	33.57	132.75	4.32	33.79
Lt. eye	44.97	12.86	37.83	1.75	18.95
Thyroid	15.83	1.84	12.63	16.95	24.75
Rt. breast	0.65	1.43	0.48	0.86	3.95
Lt. breast	0.48	3.01	0.45	0.60	4.25
Abdomen	0.24	0.21	0.21	0.21	0.32
Gonad	0.21	0.31	0.17	0.20	0.22
<b>Lateral</b>					
<i>Entrance skin dose (mGy)</i>					
Eye	58.96	72.57	51.74	397.95	31.64
Thyroid	45.93	10.11	55.97	64.91	88.21
Breast	2.58	7.54	3.01	0.96	3.86
Abdomen	0.75	0.68	0.90	0.58	1.36
Gonad	0.41	0.55	0.46	0.39	0.25
<i>Exit dose (mGy)</i>					
Eye	3.94	39.86	1.37	40.85	1.86
Thyroid	20.45	3.27	15.97	8.21	39.96
Breast	0.73	3.06	0.71	0.94	0.62
Abdomen	0.29	0.22	0.24	0.45	0.52
Gonad	0.22	0.29	0.20	0.26	0.24

Table 5.4 Effective dose values for frontal plane and lateral plane

	<b>Patient no.</b>				
	1	2	3	4	5
<b>Frontal</b>					
<b>Effective dose (mSv)</b>					
Rt. eye	35.23	5.50	11.77	44.96	35.63
Lt. eye	11.70	1.97	10.87	30.53	12.81
Thyroid	4.57	2.36	2.63	4.63	4.45
Rt. breast	0.20	0.08	0.94	0.21	0.18
Lt. breast	0.20	0.06	0.80	0.21	0.17
Abdomen	0.04	0.03	0.40	0.04	0.05
Gonad	0.12	0.09	1.44	0.13	0.14
<b>Lateral</b>					
<b>Effective dose (mSv)</b>					
Eye	2.35	22.48	0.63	2.32	2.31
Thyroid	2.53	3.83	0.19	2.16	2.05
Breast	0.14	0.05	0.19	0.11	0.11
Abdomen	0.05	0.03	0.15	0.04	0.03
Gonad	0.09	0.09	0.57	0.08	0.08

Table 5.4 Effective dose values for frontal plane and lateral plane (Continued)

	<b>Patient no.</b>				
	6	7	8	9	10
<b>Frontal</b>					
<b>Effective dose (mSv)</b>					
Rt. eye	13.45	51.21	39.80	2.61	2.05
Lt. eye	12.83	45.82	15.58	2.45	1.86
Thyroid	3.98	4.33	4.72	2.05	1.75
Rt. breast	0.14	0.21	0.28	0.10	0.09
Lt. breast	0.12	0.20	0.16	0.10	0.09
Abdomen	0.02	0.06	0.04	0.02	0.02
Gonad	0.07	0.17	0.12	0.04	0.04
<b>Lateral</b>					
<b>Effective dose (mSv)</b>					
Eye	4.48	3.83	5.13	2.32	1.86
Thyroid	1.85	1.42	2.43	1.96	1.58
Breast	0.04	0.04	0.12	0.09	0.08
Abdomen	0.01	0.01	0.05	0.03	0.02
Gonad	0.02	0.01	0.08	0.08	0.07

Table 5.4 Effective dose values for frontal plane and lateral plane (Continued)

	<b>Patient no.</b>				
	11	12	13	14	15
<b>Frontal</b>					
<b>Effective dose (mSv)</b>					
Rt. eye	50.18	46.62	33.97	60.08	33.95
Lt. eye	39.24	36.91	28.86	46.23	9.93
Thyroid	3.82	3.11	2.20	6.64	4.30
Rt. breast	0.28	0.18	0.11	0.53	0.16
Lt. breast	0.22	0.16	0.10	0.36	0.15
Abdomen	0.07	0.06	0.06	0.06	0.03
Gonad	0.19	0.16	0.15	0.17	0.10
<b>Lateral</b>					
<b>Effective dose (mSv)</b>					
Eye	5.51	4.67	3.16	7.18	2.14
Thyroid	2.75	2.00	1.46	2.94	2.00
Breast	0.14	0.11	0.08	0.11	0.11
Abdomen	0.06	0.05	0.04	0.06	0.04
Gonad	0.09	0.07	0.05	0.08	0.07

Table 5.4 Effective dose values for frontal plane and lateral plane (Continued)

	<b>Patient no.</b>				
	16	17	18	19	20
<b>Frontal</b>					
<b>Effective dose (mSv)</b>					
Rt. eye	31.71	2.01	36.65	2.09	65.50
Lt. eye	20.13	1.69	12.30	1.53	43.39
Thyroid	3.25	0.84	4.70	0.80	5.05
Rt. breast	0.10	0.03	0.21	0.03	0.35
Lt. breast	0.08	0.03	0.21	0.03	0.31
Abdomen	0.01	0.02	0.04	0.01	0.06
Gonad	0.02	0.05	0.12	0.04	0.19
<b>Lateral</b>					
<b>Effective dose (mSv)</b>					
Eye	1.35	0.59	2.15	0.68	7.49
Thyroid	0.92	0.63	1.62	0.60	3.05
Breast	0.05	0.04	0.11	0.05	0.12
Abdomen	0.01	0.01	0.04	0.01	0.07
Gonad	0.02	0.02	0.07	0.02	0.07

Table 5.4 Effective dose values for frontal plane and lateral plane (Continued)

	<b>Patient no.</b>				
	21	22	23	24	25
<b>Frontal</b>					
<b>Effective dose (mSv)</b>					
Rt. eye	8.86	18.56	15.25	59.46	22.65
Lt. eye	3.52	9.63	1.95	39.95	8.26
Thyroid	0.64	12.55	3.10	4.48	2.57
Rt. breast	0.36	0.41	0.27	0.28	0.17
Lt. breast	0.36	0.38	0.22	0.26	0.15
Abdomen	0.04	0.14	0.08	0.05	0.04
Gonad	0.13	0.20	0.09	0.16	0.10
<b>Lateral</b>					
<b>Effective dose (mSv)</b>					
Eye	3.20	1.37	6.42	6.90	4.05
Thyroid	0.45	4.16	0.38	2.75	1.59
Breast	0.36	0.16	0.07	0.10	0.09
Abdomen	0.03	0.05	0.08	0.06	0.04
Gonad	0.10	0.05	0.07	0.04	0.04

Table 5.4 Effective dose values for frontal plane and lateral plane (Continued)

	<b>Patient no.</b>				
	26	27	28	29	30
<b>Frontal</b>					
<b>Effective dose (mSv)</b>					
Rt. eye	32.09	9.24	36.05	4.64	19.29
Lt. eye	12.05	4.24	12.76	1.64	10.04
Thyroid	4.30	0.75	5.01	1.90	13.18
Rt. breast	0.17	0.41	0.21	0.06	0.45
Lt. breast	0.15	0.36	0.19	0.05	0.39
Abdomen	0.03	0.03	0.04	0.03	0.15
Gonad	0.10	0.12	0.12	0.08	0.24
<b>Lateral</b>					
<b>Effective dose (mSv)</b>					
Eye	2.95	3.63	2.59	19.90	1.58
Thyroid	2.30	0.51	2.80	3.25	4.41
Breast	0.13	0.38	0.15	0.05	0.19
Abdomen	0.04	0.03	0.04	0.03	0.07
Gonad	0.08	0.11	0.09	0.08	0.05

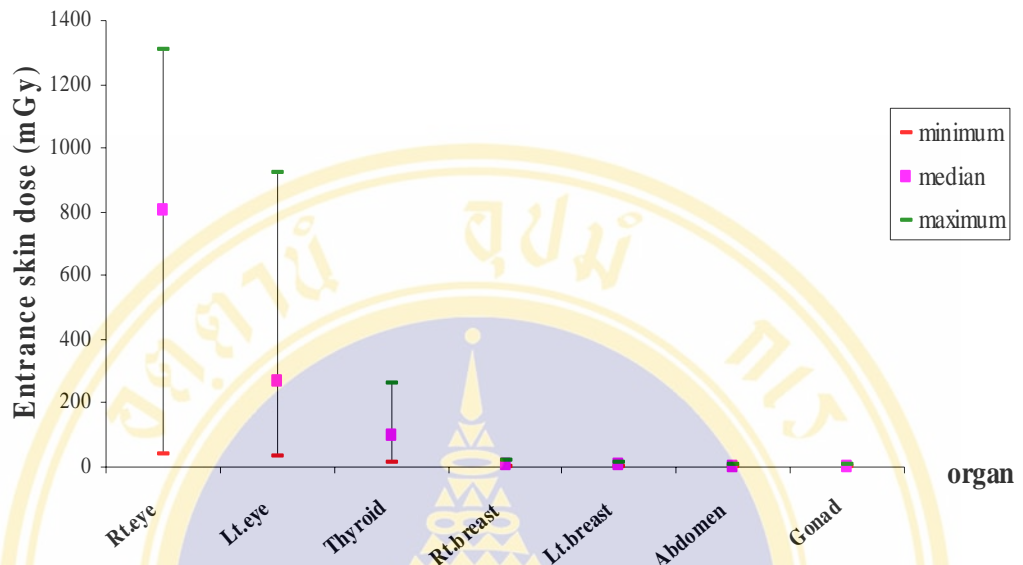


Figure 5.3 The maximum, median and minimum entrance skin dose of each organ for frontal plane

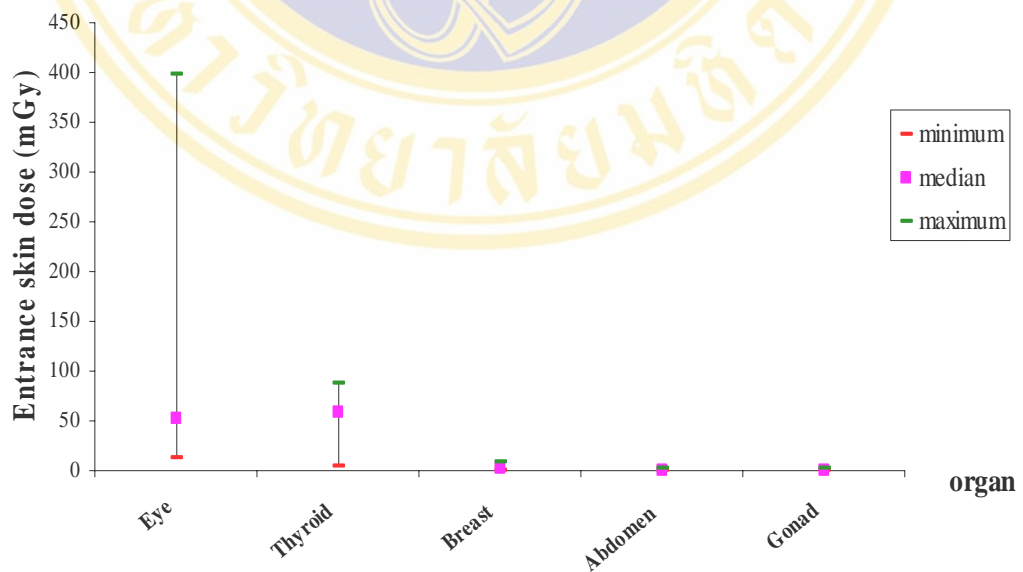


Figure 5.4 The maximum, median and minimum entrance skin dose of each organ for lateral plane

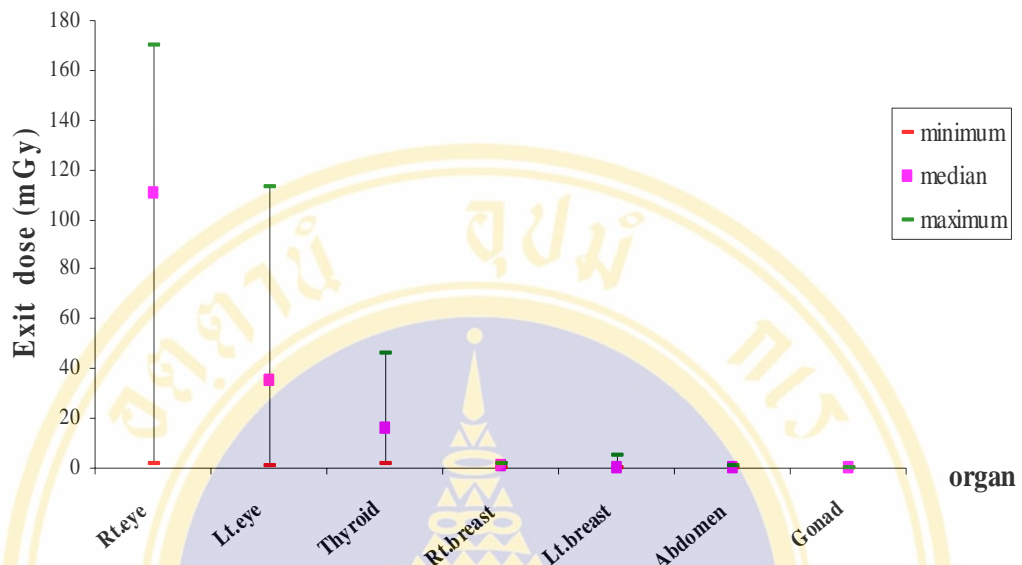


Figure 5.5 The maximum, median and minimum exit dose of each organ for frontal plane

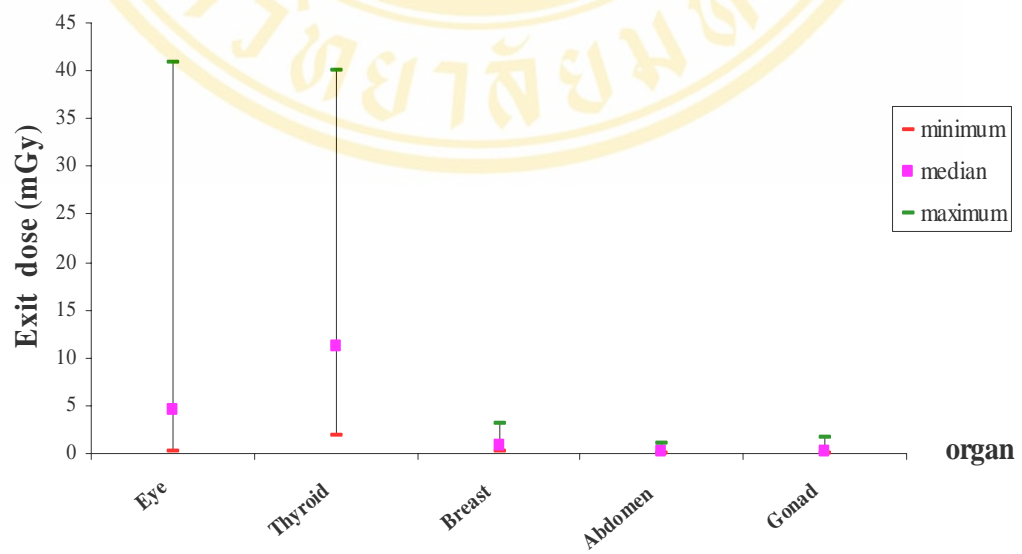


Figure 5.6 The maximum, median and minimum exit dose of each organ for lateral plane

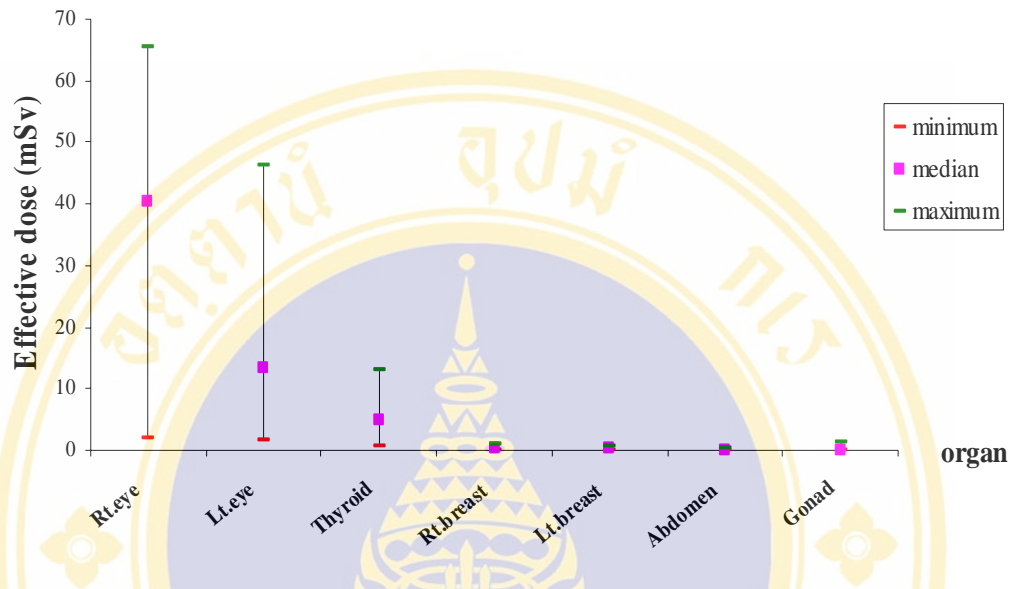


Figure 5.7 Effective dose of each organ for frontal plane

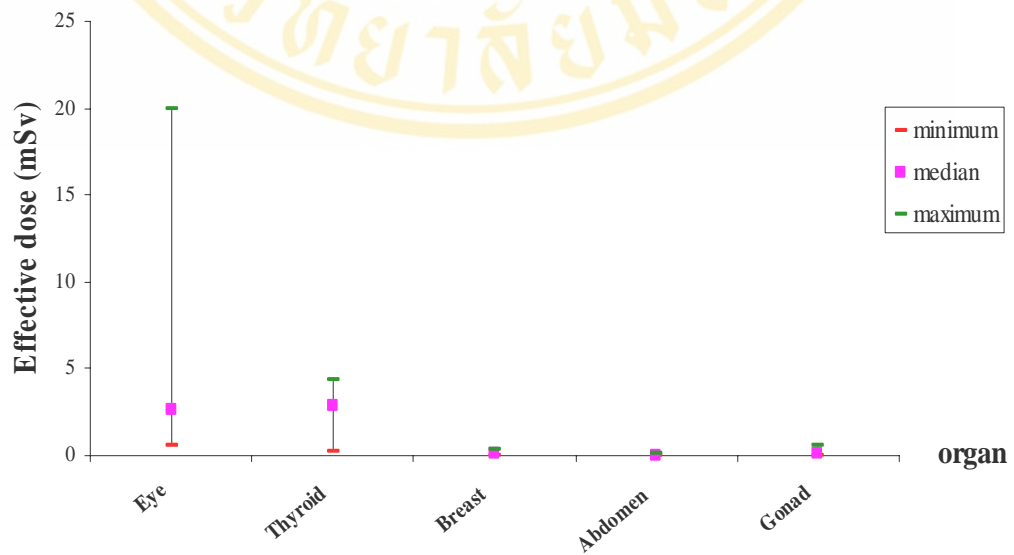


Figure 5.8 Effective dose of each organ for frontal plane

### 5.2.3 Technical factors affecting the patient dose

There are several factors affecting patient dose in endovascular embolization of AVMs. These importance factors that contributed to patient dose included tube current (mA ), peak kilovoltage (kVp), fluoroscopy time, number of radiograph, source-to-skin distance, patient-to-image intensifier distance, image magnification, patient size, grid, last image hold and collimation.

#### a. Tube current (mA )

The mA is equal to the number of electrons flowing from the cathode to the anode per unit time (x-ray produced). Therefore mA primarily affects the quantity of radiation from the tube. The quantity of radiation is directly proportional to the mA. Hence, if the mA is double, the quantity of radiation (dose to the patient) doubles.

#### b. Peak kilovoltage (kVp)

The kVp affects the penetrating power of the radiation beam. A beam produced by a high kVp is much more penetrating than a beam produced by a low kVp. This affects the dose deposited in the patient. The low kVp techniques more dose is deposited in a larger area of the patient because the photons do not have enough energy to penetrate the entire thickness of the patient. On the other hand, the high kVp techniques result in less dose deposited in the tissues because the photons have a high enough energy to penetrate the tissues.

Higher kVp, which mean a more energetic x-ray beam, result in a more penetrating beam and allow the mA to be reduced. Lower kVp require a substantially higher mA to produce acceptable images and result in a higher dose to the patient, if all other factors remain constant. The drawback to using a high kVp is loss in image contrast. Maintain the highest kVp that will provide acceptable image contrast leads to lower patient doses.

#### c. Fluoroscopy time

The amount of dose delivered to the patient is directly proportional to the amount of time that the x-ray source is energized, creating a real time image. Substantial reductions in dose may be gained by being aware of the amount of time

spent with the x-ray beam on. Use of short intermittent fluoroscopy rather than extended continuous fluoroscopy also reduces patient dose. Ultimately, keeping fluoroscopy time to minimum is the most effective way to reduce the dose to patient.

#### **d. Number of radiograph**

The number of radiographs is determined by the number of frames per second taken in the different series. Therefore low frame rate would increase time. Extended time lead to an increase patient dose.

#### **e. Source-to-skin distance**

The dose rate of a fluoroscopic x-ray beam as it exits the x-ray tube is extremely high. Increasing the source-to-skin distance reduces the dose to the patient according to the inverse square law. Maintaining the maximum possible distance between the x-ray source and the patient is one of the most effective means of reducing patient dose and minimizing potential adverse biologic effects and exposure risks.

#### **f. Patient-to-image intensifier distance**

The distance between the patient and image intensifier also has a substantial effect on patient dose. By decreasing the distance that the x-ray beam travels after exiting the patient to reach the image receptor ( ie, the image intensifier ), the dose rate of the x-ray beam can be reduced. Reduction in dose rate results in a lower cumulative dose to the patient. However, minimizing this distance also means that a larger fraction of scattered radiation will contribute to the image, possibly degrading image quality. When an x-ray changes direction because of a scatter interaction, it will not diverge as far from its original path if it has only a short distance to travel. Conversely, the farther away the image receptor is from the point of scatter, the more likely it is that the x-ray will diverge and not reach the image receptor. It is widely accepted, however, that minimizing patient-to-image intensifier distance will result in the lowest patient dose.

**g. Image magnification**

Magnification of the fluoroscopic image is possible with multified image intensifiers. Magnification degrades the image clarity on the television monitor because there is a decrease in the magnification gain that results in a decrease in the number of photoelectrons striking the output screen of the image intensifier. To keep the brightness level on the television monitor constant, the fluoroscopic mA is increased automatically and subsequently may double the original dose rate.

The ability to create a magnificatied image can be very useful and in some circumstances might be considered necessary. In almost all cases, image magnification results in hight patient dose.

**h. Patient size**

As the thickness of the area being imaged increases, the amount of radiation incident on the patient increases because adequate x-ray penetration is needed to create an acceptable image. Thicker patients or dense areas within a patient cause more of the x-ray beam to be absorbed or scattered. To maintain acceptable image brightness, contrast, and detail, the peak kilovoltage and tube current must be increased. Higher peak kilovoltage and higher tube current mean a higher dose to the patient. The backscatter factor also contributes to an increased ESD accumulates more rapidly in thick patients, making them more susceptible to radiation burns.

**i. Grid**

Use of grid in fluoroscopy reduces the amount of scattered radiation that reaches the image intensifier and yields images with improved contrast. While grids improve the contrast of the image in fluoroscopy, the removal of the grid from in front of the image intensifier can reduce the radiation dose by a factor of two or more.

**j. Last image hold**

This is a term used to describe fluoroscopic images that can be held in digital storage and subsequently displayed on the television monitor without the need for continuous fluoroscopy. Systems with the last image hold feature reduce the dose to the patient by reducing the total fluoroscopic time.

### **k. Collimation**

Fluoroscopy collimations are important in considerations of patient dose. Because extended fluoroscopy times may be used in fluoroscopy, areas adjacent to the location of clinical interest can receive substantial doses. This potential overexposure is easily remedied by using the smallest field possible to image only the area of interest. Proper collimation also reduces the contribution of scattered radiation and leads to higher quality images.

A quantitative understanding of the relationship between patient doses and exposure factor variation is therefore important to help operators make the best use of digital imaging equipment. Improvements in imaging performance should require the modification of those radiographic technique factors that minimize the patient radiation risk. If it is possible to reduce exposure factors without adverse affect diagnostic performance and image quality. Technical factors should be modified to maximize patient dose saving.

In fluoroscopy mode, fluoroscopy time was a major parameter that influence the patient dose. Concerning the radiographs, the influence of the number of radiographs to the total dose dominates in some cases than the other parameters. However, increased these parameters could increase in patient dose.

From the results of the dose measurement in 30 patients conclude that the contribution of the radiographs to the total dose is much higher than the contribution of fluoroscopy. The large contribution of the radiographs to the total dose is due to the current for radiography is much higher than for fluoroscopy. Therefore, special attention should be given to the radiographs in the scope of optimizing patient doses.

## CHAPTER VI

### CONCLUSION

Dosimetric evaluations of endovascular embolization of AVMs are difficult and time consuming, because the exposure conditions vary widely even during examination. However, The direct measurement by using TLDs is the best way to obtain information about skin dose. Since the risk associated with skin dose is deterministic effect.

The dose measurement in this study appear higher than in the literatures. Although the maximum skin doses present in this study was not high enough to cause concern about induction of deterministic effects. However, it is important to monitor and note the effect that can occur in some cases such as repeat embolization perform in the same patient in overlapping periods of treatment in order to ensure the patient dose is below the relevant thresholds. While the deterministic effect and stochastic effect are likely to result in a detriment to health, it is important to note that the radiation risk is expected to be vary small in comparison to the benefit to the individual undergoing the endovascular embolization of AVMs, given that the latter is performed to decrease the chance of future or further neurologic damage, to improve the quality of life of the patient or to save lives. As such, the risk benefit ratio to the exposed individual is likely to be small.

## REFERENCES

1. Balter S, Shope TB. Syllabus: A categorical course in physics: physical and technical aspects of angiography and interventional radiology. 81<sup>st</sup> Scientific Assembly, 1995:1-258.
2. Vinuela F. Interventional Neuroradiology. New York: Raven, 1992:345-62.
3. Connors JJ, Wojak JC. Interventional Neuroradiology. In: Strategies and Practical Techniques. Philadelphia: W. B. Saunders, 1999:173-94.
4. Berthelsen B, Cederblad A. Radiation doses to patients and personnel involved in embolization of intracerebral arteriovenous malformations. *Acta Radiol* 1991;32:492-497.
5. Gkanatsios NA, Huda W, Peters KR, and Freeman JA. Evaluation of an on-line patient exposure meter in neuroradiology. *Radiology* 1997; 193:642-44 .
6. Ruiz CR, Garcia GJ, Diaz FJ, and Hernandez AJ. Estimation of effective dose in some digital angiographic and interventional procedures. *Brit. J. Radiol* 1998 ;71:42-7.
7. Faulkner K, Teunen D. Radiation protection in interventional radiology. *British Institute of Radiology* 1995:139-45.
8. Faulkner K, Teunen D. Justification in radiation protection. *Brit. J. Radiol* 1998:512-21.
9. International Commission on Radiological Protection. Recommendations of the International Commission on Radiological Protection. ICRP report 26 1997.
10. International Commission on Radiological Protection. Recommendations of the International Commission on Radiological Protection. ICRP report 60 1991.
11. National Council on Radiation Protection and Measurements. Recommendations on Limits for Exposure to Ionizing Radiation. NCRP report 90 1987.
12. Zankl M, Petoussi N, and Drexler G. Effective dose and effective dose equivalent

- : The impact of the new ICRP definition for external photon irradiation. Health Phys 1992;62:395-99.
13. Steven BD, Elwin RT. Practical radiation protection and applied radiobiology. 2<sup>nd</sup> ed. Philadelphia , 1999:47,78-9,190-91.
  14. Huda W, Sandison GA. Estimation of mean organ dose in diagnostic radiology from rando phantom measurements. Health Phys 1984:47,463-67.
  15. International Commission on Radiological Protection. Report of the Task Group on Reference Man. ICRP report 23 1975.
  16. Wagner LK, Archer BR. Minimising Risks from Fluoroscopic X Rays. 2<sup>nd</sup> ed. Texas: The Woodlands, 1998.
  17. Wagner LK, Archer BR. Management of patient skin dose in fluoroscopically guided interventional procedures. J. Vasc. Intervent. Radiol 2000;11: 25–34.
  18. Gill JR. Overexposure of patients due to malfunctions or defects in radiation equipment. Rad. Prot. Dosim 1992: 43, 257–260.
  19. National Council on Radiation Protection and Measurements. Limitation of Exposure to Ionizing Radiation. NCRP report 116 1993. .
  20. Busuoli G. Applied Thermoluminescence Dosimetry. Brussels and Luxembourg : Eds M Oberhofer and A Scharmann 1981:91-95.
  21. Wu. DK, Sun FY and Dai HCA. High Sensitivity LiF Thermoluminescent dosimeter- LiF( Mg,Cu,P ). Health Phys. 1984;46:1063-67.
  22. DeWerd LA, Cameron JR, Wu DK and Das IJ. Characteristics of a New Dosemeter Material; LiF( Mg,Cu,P ) . Radiat. Prot. Dosim 1984;6:350-52.
  23. Mckeever SWS, Moscovitch M, and Townsend PD. Thermoluminescence Dosimetry Materials : Properties and Uses. Nuclear Technology Publishing, Ashford , UK , 1995 .
  24. William JR., Thwaites DI. Radiotherapy physics : in practice. 2<sup>nd</sup> ed . New Yoak: Oxford university press,2000:221-228.
  25. Shinde SS, Dhabekar B, and Bhatt BC. Preparation and characteristics of LiF: Mg,Cu,P thermoluminescent phosphor for personnel monitoring. Radiat. Prot. Dosm.1984;6(1-4):350-2.
  26. Chandra B, Lakshmanan AR, Bhatt RC, Vohra KG. Annealing and reuseability characteristics of LiF(Mg,Cu,P) TLD phosphor. Radiat. Prot. Dosm.1982;

3(3):161-7.

27. Theodorakou C and Horrocks JA. A study on radiation doses and irradiated in cerebral embolisation. *Brit. J. Radiol* 2003;76:546-52.
28. Mooney RB, McKinstry CS and Kamel HAM. Absorbed dose and deterministic effects to patients from interventional neuroradiology. *Brit. J. Radiol* 2000;73:745-51.
29. Thomas J O' Dea , Richard AG and Russell RE. The potential for radiation induced skin damage in interventional neuroradiological procedures: A review of 522 cases using automated dosimetry. *Med Phys* 1999;26: 2027-33.
30. Roshan SL , Raghuram L, Ipeson PK and Raj DV. Evaluation of radiation risk and work practices during cerebral interventions. *J Radiol Prot* 2003;23:327-36.
31. Gkanatsios NA, Huda W and Peters KR. Adult patient doses in interventional neuroradiology. *Med Phys* 2002;29:717-23.

## BIOGRAPHY



**NAME** Miss Wanlapa Promsiri

**DATE OF BIRTH** 7 July 1975

**PLACE OF BIRTH** Udornthani, Thailand

**INSTITUTIONS ATTENDED** Mahidol University,1996 :Bachelor of  
Science (Radiological Technology)  
Mahidol University, 2003 :Master of  
Science (Medical Physics)

**HOME ADDRESS** 234/264 Unifortune Mansion ,B2building  
10<sup>th</sup> floor , Pattanakarn Road , Prawet ,  
Bangkok, Thailand 10250